

---

# PRECISION AUTOTUNING FOR LINEAR SOLVERS VIA CONTEXTUAL BANDIT-BASED RL

---

PREPRINT

 **Erin Carson\***

Charles University  
Prague, Czech  
carson@karlin.mff.cuni.cz

 **Xinye Chen**

Sorbonne Université, CNRS, LIP6  
Paris, France  
xinye.chen@lip6.fr

April 1, 2026

## ABSTRACT

We propose a reinforcement learning (RL) framework for adaptive precision tuning for linear solvers, which can be extended to general algorithms. The framework is formulated as a contextual bandit problem and solved using incremental action-value estimation with a discretized state space to select optimal precision configurations for computational steps, balancing precision and computational efficiency. To verify its effectiveness, we apply the framework to iterative refinement for solving linear systems  $Ax = b$ . In this application, our approach dynamically chooses precisions based on calculated features from the system while maintaining acceptable accuracy and convergence. In detail, an action-value estimator takes discretized features (e.g., approximate condition number and matrix norm) as input and outputs estimated action values, from which a policy selects the actions (chosen precision configurations for specific steps), optimized via an  $\epsilon$ -greedy strategy to maximize a multi-objective reward to balance accuracy and computational cost. Empirical results demonstrate effective precision selection, reducing computational cost while maintaining accuracy comparable to double-precision baselines. The framework generalizes to diverse out-of-sample data and provides insights into applying RL precision selection to other numerical algorithms, advancing mixed-precision numerical methods in scientific computing. To the best of our knowledge, this is the first work on precision autotuning with RL with verification on unseen datasets.

**Keywords** mixed-precision computing, reinforcement learning, precision tuning, linear solvers, AI for numerical methods

## 1 Introduction

Floating-point arithmetic [21] is widely used in machine learning and scientific computing. With the rapid development of large language models [5, 20, 32] as well as large-scale GPU computing [24, 29], numerical calculations and algorithm deployment with extensive use of floating-point arithmetic are often accompanied by a substantial increase in energy use. Therefore, using reduced-precision arithmetic in algorithms is typically required in many intensive computing kernels due to its lower communication, faster arithmetic, and energy efficiency. Seven commonly-used floating-point formats are referenced in Table 1. The NVIDIA A100 achieves up to 312 TFLOPS with half precision (FP16/BF16), 156 TFLOPS with TF32, and 9.7 TFLOPS with FP64, yielding an approximate  $32\times$  speedup for low-precision formats. Further, the NVIDIA H100 (NVIDIA’s Hopper architecture) achieves up to 624 TFLOPS with fp8, offering an approximate  $64\times$  speedup versus FP64 [27, 25]. The work [25] demonstrates that the FP8 formats E4M3 and E5M2 can in some cases match FP16 accuracy with reduced compute and memory costs.

---

\*Supported by the Charles University Research Centre program No. UNCE/24/SCI/005 and the European Union (ERC, inEXASCALE, 101075632). Views and opinions expressed are those of the authors only and do not necessarily reflect those of the European Union or the European Research Council. Neither the European Union nor the granting authority can be held responsible for them.

However, reduced-precision arithmetic often brings increased rounding errors and numerical instability, which can compromise the results of computations, especially at large scale [23]. The idea behind mixed-precision algorithms is to design an algorithm that combines low and high precision arithmetic while retaining an acceptable level of accuracy, which remains a major obstacle in modern approximate computing paradigms [3, 36]. Accordingly, many theoretical analyses of rounding error, mixed-precision algorithms [10, 11, 12, 10, 2], and precision tuning tools [31, 15] have been developed, which aim to achieve a balance between precision loss and arithmetic speedup.

Theoretical analyses of the use of multiprecision arithmetic and mixed-precision algorithms have been extensively conducted in the context of iterative refinement [12, 2], least squares problems [19, 12], and GMRES [22]. For example, iterative refinement can be executed in three precisions, but the convergence is only theoretically guaranteed for a limited range of problems, which can be overly restrictive in practice [28]. As such, one can instead use precision tuning tools to find a suitable mixed-precision approach. Existing tools typically require running the program multiple times via trial-and-error, and the scalability and general ability are not verified, so they are either limited to small or medium-scale programs or suffer from efficiency issues. An ideal case for a precision tuning tool or method is to fit the model in a limited number of training sets and learn the key features that can be used to infer mixed-precision configurations for new unseen data. These challenges need to be addressed to reduce the dependency on programmer efforts.

Table 1: Key parameters of seven floating-point formats;  $u$  denotes the unit-roundoff corresponding to the precision,  $x_{\min}$  denotes the smallest positive normalized floating-point number,  $x_{\max}$  denotes the largest floating-point number,  $t$  denotes the number of binary digits in the significand (including the implicit leading bit),  $e_{\min}$  denotes exponent of  $x_{\min}$ , and  $e_{\max}$  denotes exponent of  $x_{\max}$ .

	$u$	$x_{\min}$	$x_{\max}$	$t$	$e_{\min}$	$e_{\max}$
bfloat16 (BF16)	$3.91 \times 10^{-3}$	$1.18 \times 10^{-38}$	$3.39 \times 10^{38}$	8	-126	127
half precision (FP16)	$4.88 \times 10^{-4}$	$6.10 \times 10^{-5}$	$6.55 \times 10^4$	11	-14	15
TensorFloat-32 (TF32)	$9.77 \times 10^{-4}$	$1.18 \times 10^{-38}$	$1.70 \times 10^{38}$	11	-126	127
single (FP32)	$5.96 \times 10^{-8}$	$1.18 \times 10^{-38}$	$3.40 \times 10^{38}$	24	-126	127
double (FP64)	$1.11 \times 10^{-16}$	$2.23 \times 10^{-308}$	$1.80 \times 10^{308}$	53	-1022	1023

A contextual bandit (also known as a multi-armed bandit with context) is a simplified reinforcement learning (RL) problem where the agent makes decisions based on the current context (i.e., state) without considering the future contexts or rewards of its actions; in other words, the agent optimizes for one-step (immediate) reward rather than long-term cumulative reward. In this paper, we propose a general framework for applying RL for precision selection in general numerical algorithms, formulated as a contextual bandit problem due to the independence of problem instances and the single decision per instance. This is the first work to formally define the use of RL for precision selection in any algorithm. The framework uses an epsilon-greedy strategy, controlled by a decaying epsilon determined by training episodes, to select precision levels for the prespecified algorithm steps, treating precision choices as a multi-armed bandit problem within a RL environment. The epsilon parameter balances exploration and exploitation, starting high to encourage diverse precision selections and decaying over time to favor optimal choices. We believe this framework enables at least three advantages:

1. Identifying the precision level required for user-specific computational steps in terms of hand-crafted features or low computational complexity features modeled from linear systems;
2. Finding salient features of the linear systems (e.g., condition number, matrix norm, non-zero values, diagonal dominance) to determine the reduced-precision configurations;
3. Being able to inference reduced- and mixed-precision configurations for unseen datasets.

We apply this framework to the GMRES-based iterative refinement (GMRES-IR) method [10] to verify the effectiveness and generalization ability of RL for precision selection, aiming to achieve a trade-off between the use of low precision and accuracy. The framework is particularly suited for scenarios with limited training data and is designed to generalize to new data, and can be easily implemented in an online learning routine to avoid model retraining.

The rest of the paper is structured as follows. Section 2 discusses the existing literature on precision autotuning as well as its pros and cons, and a comparison with our work. Section 3 presents our general framework for precision selection; to verify its effectiveness, we use the GMRES-IR method, a well-studied mixed-precision method, as a case study detailed in Section 4. Section 5 presents the experiments and empirical results on both dense and sparse matrices under varying condition numbers and sparsity. Section 7 discusses limitations as well as future work.

## 2 Related Work

There exist a variety of theoretical rounding error analysis of basic mixed-precision algorithms aimed at understanding the underlying arithmetic behavior; see the survey [1] and references therein. However, for real-world problems, which can be more complex, the scientific community typically uses more general approaches such as precision tuning tools, which operate at program compile time and runtime, immediately resulting in reduced-precision programs produced automatically. In this section, we briefly review existing approaches for the analysis of mixed-precision algorithms and automated precision tuning that are closely related to our method.

Theoretical analysis aims to design reduced-precision settings for specific steps and analyze their rounding error so that the reduced-precision arithmetic can be used safely under certain assumptions to retain algorithm accuracy and numerical stability. Analyses in [35] and [26] demonstrate that in standard iterative refinement, residuals computed in extra precision (typically twice the working precision) can guarantee the convergence of the relative error to the level of the working precision if the matrix  $A$  has a condition number safely less than the reciprocal of the unit-roundoff,  $u$ . More recently, [10] found that it is possible to produce solutions to iterative refinement with normwise relative error of order  $u$  for systems with condition numbers of order  $u^{-1}$  or larger by using a GMRES-based approach called GMRES-IR (see Algorithm 2). The authors extended this work in [11] to develop a general analysis of iterative refinement using up to three difference precisions, as well as a general solver. This work shows that, depending on constraints on the condition number  $\kappa(A)$ , the most expensive part of the computation can often be carried out entirely in low precision without harming the accuracy. However, to obtain theoretical results such as these, a great amount of effort is needed, and the analysis often relies on knowledge about the problem, e.g., the condition number, which may not be readily available in practice. To circumvent these obstacles, one can switch to precision tuning tools that operate during compile time and runtime; see the survey [13] and references therein.

Another approach is to use an automated precision tuning method. Such methods, built upon the software level via static and dynamic analysis tools [3], can obtain suitable reduced-precision settings through trial and error. The search-based tool Precimonious [31] uses high-performance dynamic programming approaches, which achieve a potentially lower precision setting for the program via Delta Debugging of the space of possible floating-point configurations within the target accuracy. Further, HiFPTuner [15] (High-level Floating-Point Tuner) operates at the source level to automatically tune the floating-point precision via profiling floating-point operations and estimating the numerical impact of the reduced-precision program. CRAFT [23] builds reduced-precision configurations of floating-point programs based on the Dyninst binary instrumentation framework [7], and uses an automatic search process that identifies the precision-level sensitivity of various parts of an application. Search-based tools for finding a low-precision configuration typically require a dramatic increase in computational cost as the number of variables increases, and do not scale well to large programs. To further reduce the runtime of precision tuning, Blame Analysis [30] is devoted to executing a program once, analyzing floating-point instructions to determine the minimum precision required for each operand, reducing the search space of Precimonious and improving scalability. PyFloT [6] automates mixed-precision tuning for HPC applications by leveraging runtime profiling, instruction-level granularity, and temporal locality to learn numerical behavior and recurring patterns in instruction execution. FPLearner [34] leverages a graph representation learning technique to predict the performance and accuracy of a mixed-precision program, which can then be used to accelerate dynamic precision tuning by reducing the number of program runs.

The aforementioned methods target floating-point programs, and the general ability to handle unseen data remains unverified. Our proposed method operates in a different setting. It proceeds by modeling the rewards associated with multiple objectives and user-defined states (characteristics for the method to be defined in mixed-precision) and learning via several rounds of training on a specific, limited dataset. This approach can be generalized to a variety of unseen testing data. To the best of our knowledge, we are the first to present a work on precision autotuning for numerical algorithms that has verified generalization performance. In the following section, we will detail our framework and methodology for using RL to intelligently select precision configurations.

## 3 A General RL Framework for Precision Selection

We formalize the precision selection problem for a general algorithm  $\mathcal{M}$  for solving linear systems as a contextual bandit, where an agent dynamically selects precision configurations for computational steps based on features of the problem instance. This framework is summarized in Figure 1 and can easily be performed in an online learning routine. It intelligently optimizes the trade-off between numerical accuracy and computational efficiency, leveraging RL to adapt to diverse problem characteristics.

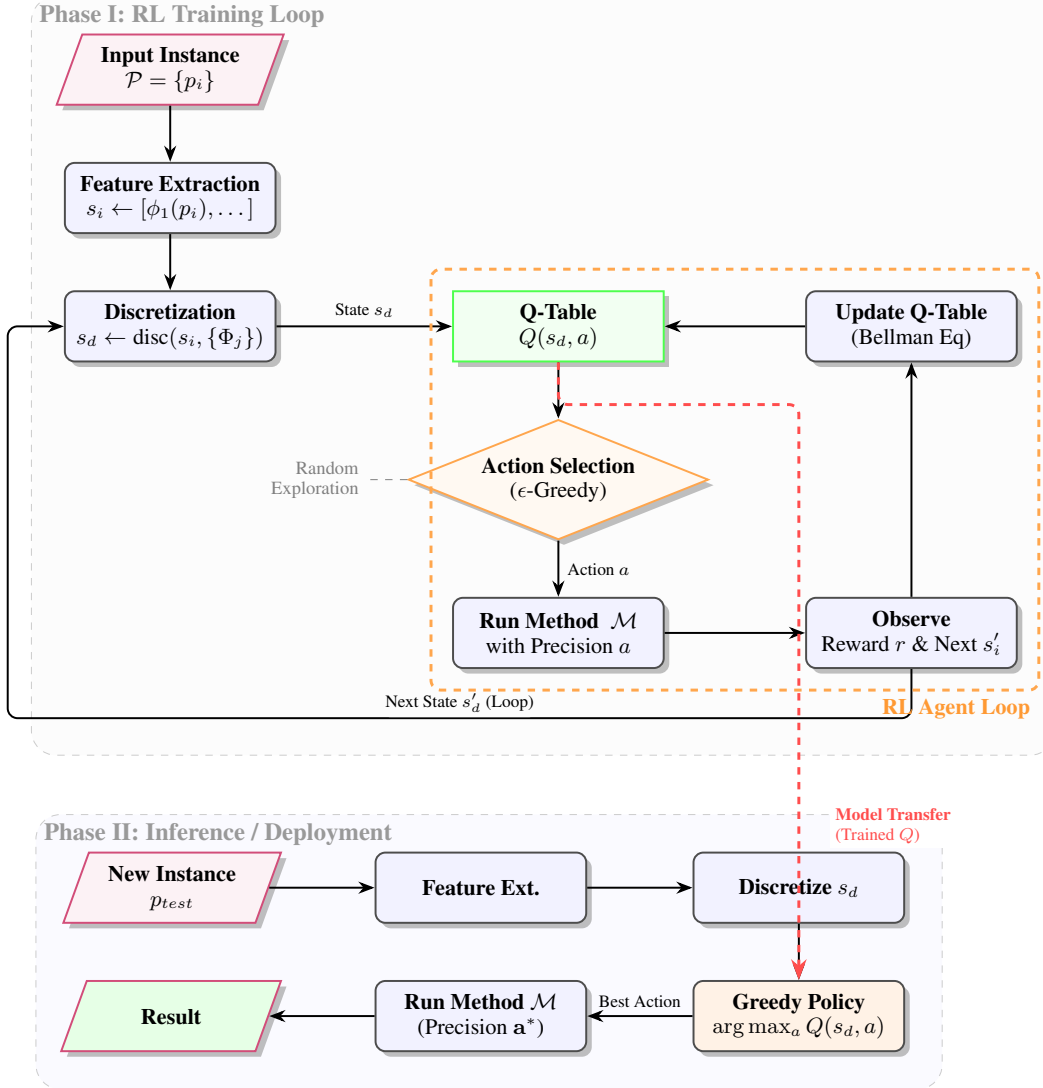


Figure 1: Schematic of RL Framework: Phase I (top) depicts the iterative training loop where the agent updates the Q-table. Phase II (bottom) shows the inference workflow using the trained RL model.

### 3.1 Contextual Bandit Formulation

Consider a numerical algorithm or method  $\mathcal{M}$  designed to solve a problem instance  $p \in \mathcal{P}$ , where  $\mathcal{P}$  denotes the set of problem instances (e.g., linear systems  $Ax = b$ ). The method comprises  $k$  computational steps, each requiring a precision choice from a finite set  $\mathcal{A}_i = \{u_{i,1}, u_{i,2}, \dots, u_{i,m}\}$ , for  $i = 1, \dots, k$ , where  $m = |\mathcal{A}_i|$  is the number of available precisions. The action space is the Cartesian product:

$$\mathcal{A} = \mathcal{A}_1 \times \mathcal{A}_2 \times \dots \times \mathcal{A}_k, \quad (1)$$

with cardinality  $|\mathcal{A}| = m^k$ . An action is a tuple  $\mathbf{a} = (a_1, a_2, \dots, a_k) \in \mathcal{A}$ , where  $a_i \in \mathcal{A}_i$  specifies the precision for the  $i$ -th computational step. To reduce the computational complexity and simplify the problem, we assume  $|\mathcal{A}_1| = |\mathcal{A}_2| = \dots = |\mathcal{A}_k|$ .

The contextual bandit is defined by:

- **Context** ( $s \in \mathcal{S}$ ): A feature vector describing the problem instance  $p$ , i.e.,  $s = [\phi_1(p), \phi_2(p), \dots, \phi_d(p)] \in \mathbb{R}^d$ , where  $\phi_j : \mathcal{P} \rightarrow \mathbb{R}$  are features capturing properties such as condition number, sparsity, matrix norm, or matrix size.

- **Action** ( $\mathbf{a} \in \mathcal{A}$ ): A precision configuration  $\mathbf{a} = (a_1, \dots, a_k)$ , where  $a_i$  determines the precision for the  $i$ -th step.
- **Reward** ( $r(s, \mathbf{a})$ ): A scalar evaluating the performance of  $\mathcal{M}$  on instance  $p$  with action  $\mathbf{a}$ , defined as a weighted sum of  $J$  objectives:

$$r(s, \mathbf{a}) = \sum_{j=1}^J w_j f_j(s, \mathbf{a}), \quad (2)$$

where  $f_j : \mathcal{S} \times \mathcal{A} \rightarrow \mathbb{R}$  are objective functions (e.g., accuracy, computational cost, convergence indicators), and  $w_j > 0$  are weights balancing these objectives.

The goal is to learn a policy  $\pi : \mathcal{S} \rightarrow \Delta(\mathcal{A})$ , where  $\Delta(\mathcal{A})$  is the probability simplex over  $\mathcal{A}$  that maximizes the expected reward over a distribution of problem instances  $\mathcal{D}$ :

$$J(\pi) = \mathbb{E}_{s \sim \mathcal{D}, \mathbf{a} \sim \pi(\cdot|s)} [r(s, \mathbf{a})].$$

### 3.2 Learning with Discretized Context Space

To learn the policy  $\pi$  for determining precision choice, we employ a contextual bandit learning paradigm, discretizing the continuous state space  $\mathcal{S}$  into a finite set to manage computational complexity. For each feature  $\phi_j$  ( $j = 1, \dots, d$ ), we define bins  $\Phi_j = \{b_{j,1}, b_{j,2}, \dots, b_{j,n_j}\}$ , where  $n_j$  is the number of bins (e.g., logarithmic bins for condition number and norm, linear bins for sparsity and diagonal dominance). The discretized state space is:

$$\mathcal{S}_d = \Phi_1 \times \Phi_2 \times \dots \times \Phi_d, \quad (3)$$

with cardinality  $|\mathcal{S}_d| = \prod_{j=1}^d n_j$ . A state  $s_d \in \mathcal{S}_d$  is obtained by mapping the continuous context  $s = [\phi_1, \dots, \phi_d]$  to a discrete index via binning:

$$s_d = \text{discretize}(s) = (\text{bin}(\phi_1(p)), \dots, \text{bin}(\phi_d(p))), \quad (4)$$

where  $\text{bin}(\cdot)$  assigns each feature to the nearest bin in  $\Phi_j$ , with clipping to ensure indices remain within bounds.

To handle the combinatorial action space  $\mathcal{A} = \mathcal{A}_1 \times \dots \times \mathcal{A}_k$  with cardinality  $|\mathcal{A}| = m^k$ , we directly learn a tabular action-value function

$$Q : \mathcal{S}_d \times \mathcal{A} \rightarrow \mathbb{R},$$

where  $Q(s_d, \mathbf{a})$  estimates the expected reward obtained by applying the precision configuration  $\mathbf{a} = (a_1, \dots, a_k) \in \mathcal{A}$  to the solver under discretized state  $s_d \in \mathcal{S}_d$ .

This formulation treats each precision configuration as a distinct action, capturing the joint effect of precision choices across all computational steps. The resulting Q-table has size  $|\mathcal{S}_d| \cdot |\mathcal{A}| = |\mathcal{S}_d| \cdot m^k$ , which can become prohibitively large as the number of steps  $k$  or precision levels  $m$  increases.

In the following subsection, we introduce a structured reduction of the action space to mitigate this exponential growth while preserving numerically meaningful configurations.

During training, the policy selects actions using an epsilon-greedy strategy to balance exploration and exploitation. For each episode, given a discretized state  $s_d \in \mathcal{S}$ , the agent selects an action  $\mathbf{a} \in \mathcal{A}$ , where  $\mathbf{a} = (u_1, u_2, \dots, u_k)$  represents a tuple of precisions. The set  $\mathcal{A}$  contains (valid) precision combinations. The probability of selecting an action  $\mathbf{a}$  is given by:

$$\pi(\mathbf{a}|s_d) = \begin{cases} 1 - \epsilon + \epsilon/|\mathcal{A}| & \text{if } \mathbf{a} = \arg \max_{\mathbf{a}' \in \mathcal{A}} Q(s_d, \mathbf{a}'), \\ \epsilon/|\mathcal{A}| & \text{otherwise,} \end{cases} \quad (5)$$

where  $\epsilon \in [0, 1]$  is the exploration parameter, initialized to  $\epsilon_0 = 1.0$  and decayed as  $\epsilon \leftarrow \max(\epsilon_{\min}, 1.0 - \text{episode}/\text{total\_episodes})$  with a minimum exploration rate  $\epsilon_{\min}$ .

After selecting an action  $\mathbf{a}$ , the environment applies the mixed-precision algorithm to the linear system  $\mathbf{A}\mathbf{x} = \mathbf{b}$ , yielding a reward  $R(s_d, \mathbf{a})$  based on accuracy, precision usage, convergence, and iteration count. The Q-table is updated with a one-step:

$$Q(s_d, \mathbf{a}) \leftarrow Q(s_d, \mathbf{a}) + \alpha (R(s_d, \mathbf{a}) - Q(s_d, \mathbf{a})), \quad (6)$$

where  $\alpha \in (0, 1]$  is the learning rate. The Q-values are not necessarily clipped in the implementation, relying on the reward function to manage numerical stability.

During inference, the agent selects the action that maximizes the Q-value for the given state:

$$\mathbf{a}^* = \arg \max_{\mathbf{a}' \in \mathcal{A}} Q(s_d, \mathbf{a}'). \quad (7)$$

**Algorithm 1** Contextual Bandit Framework for Precision Selection

- 
- 1: **Input:** Training instances  $\mathcal{P} = \{p_1, \dots, p_N\}$ , numerical method  $\mathcal{M}$ , precision sets  $\{\mathcal{A}_i\}_{i=1}^k$ , reward function  $r$ , episodes  $T$ , learning-rate schedule  $\alpha_t$ , exploration rate  $\epsilon$ , bin sets  $\{\Phi_j\}_{j=1}^d$
  - 2: Construct the joint action space  $\mathcal{A} = \mathcal{A}_1 \times \dots \times \mathcal{A}_k$
  - 3: Initialize a tabular action-value estimator  $Q(s_d, \mathbf{a})$  for all  $s_d \in \mathcal{S}_d$  and  $\mathbf{a} \in \mathcal{A}$
  - 4: Initialize visit counts  $N(s_d, \mathbf{a}) \leftarrow 0$  for all  $s_d \in \mathcal{S}_d$  and  $\mathbf{a} \in \mathcal{A}$
  - 5: **for** episode  $t = 1$  to  $T$  **do**
  - 6:     **for** each instance  $p_i \in \mathcal{P}$  **do**
  - 7:         Compute context  $s_i \leftarrow [\phi_1(p_i), \dots, \phi_d(p_i)]$
  - 8:         Discretize context  $s_d \leftarrow \text{discretize}(s_i, \{\Phi_j\})$
  - 9:         Select action  $\mathbf{a} \in \mathcal{A}$  using an  $\epsilon$ -greedy policy:
 
$$\mathbf{a} \leftarrow \begin{cases} \text{a uniformly random action in } \mathcal{A}, & \text{with probability } \epsilon, \\ \arg \max_{\mathbf{a}' \in \mathcal{A}} Q(s_d, \mathbf{a}'), & \text{with probability } 1 - \epsilon \end{cases}$$
  - 10:         Run  $\mathcal{M}$  with precision configuration  $\mathbf{a}$  on  $p_i$
  - 11:         Observe reward  $r_i \leftarrow r(s_d, \mathbf{a})$
  - 12:         Update visit count:  $N(s_d, \mathbf{a}) \leftarrow N(s_d, \mathbf{a}) + 1$
  - 13:         Set learning rate, e.g.,
 
$$\alpha \leftarrow \frac{1}{N(s_d, \mathbf{a})}$$
  - 14:         Update the tabular action-value estimator:
 
$$Q(s_d, \mathbf{a}) \leftarrow Q(s_d, \mathbf{a}) + \alpha(r_i - Q(s_d, \mathbf{a}))$$
  - 15:     **end for**
  - 16:     Update  $\epsilon$
  - 17: **end for**
  - 18: **Inference:** For a new instance  $p$ , compute  $s = [\phi_1(p), \dots, \phi_d(p)]$ , discretize  $s_d = \text{discretize}(s, \{\Phi_j\})$ , and select
 
$$\mathbf{a}^* = \arg \max_{\mathbf{a} \in \mathcal{A}} Q(s_d, \mathbf{a}).$$
  - 19: Apply  $\mathcal{M}$  with precision configuration  $\mathbf{a}^*$
- 

Our learning framework for precision selection is formulated as a contextual bandit over a discretized context space. For each problem instance  $p = (A, b) \in \mathcal{P}$ , we compute a feature vector  $s = [\phi_1(p), \dots, \phi_d(p)]$  and map it to a discrete context  $s_d \in \mathcal{S}_d$ . The agent then selects a joint precision configuration  $\mathbf{a} = (a_1, \dots, a_k) \in \mathcal{A}$  for the  $k$  computational steps of the solver. After executing the mixed-precision algorithm with action  $\mathbf{a}$ , the environment returns a scalar reward  $r(s_d, \mathbf{a})$  that balances numerical accuracy, computational cost, convergence behavior, and iteration count.

To estimate the expected reward of each state-action pair, we maintain a single tabular function  $Q(s_d, \mathbf{a})$ . During training, actions are sampled using an  $\epsilon$ -greedy exploration rule, and the table is updated using the incremental estimator

$$Q(s_d, \mathbf{a}) \leftarrow Q(s_d, \mathbf{a}) + \alpha_t(s_d, \mathbf{a})(r(s_d, \mathbf{a}) - Q(s_d, \mathbf{a})).$$

In the inference phase, for a new instance  $p$ , the context  $s$  is computed and discretized to  $s_d$ , and the precision configuration is selected greedily as

$$\mathbf{a}^*(s_d) = \arg \max_{\mathbf{a} \in \mathcal{A}} Q(s_d, \mathbf{a}).$$

Using a single Q-table over the reduced joint action space preserves the interaction among precision choices across different computational steps while keeping the learning problem tractable. The feature-based context enables the framework to adaptively select numerically effective and computationally efficient precision configurations, as validated in the numerical experiments in Section 5.

Our RL learning framework optimizes both arithmetic efficiency (by favoring lower-precision steps) and solver performance (e.g., convergence and accuracy). In Section 4, we will apply this framework to GMRES-IR, and detail how we model the reward function based on the earnings and cost for the steps following low precision.

**Theoretical Justification of Discretization** Our contextual bandit framework relies on the discretization of the continuous context space  $\mathcal{S}$  into a finite set  $\mathcal{S}_d$ . This raises the question of how much optimality is lost due to this

approximation. We provide a bound below showing that, under a mild smoothness assumption on the expected reward, the performance loss induced by discretization is controlled by the granularity of the bins.

**Assumption 1** (Lipschitz continuity of the expected reward). Let  $\mu(s, \mathbf{a}) := \mathbb{E}[r(s, \mathbf{a})]$  denote the expected reward. We assume, for all  $\mathbf{a} \in \mathcal{A}$ , there exists a constant  $L > 0$  such that

$$|\mu(s, \mathbf{a}) - \mu(s', \mathbf{a})| \leq L\|s - s'\|, \quad \forall s, s' \in \mathcal{S}. \quad (8)$$

**Proposition 1** (Discretization error bound). Let  $s \in \mathcal{S}$  be a continuous context, and let  $s_d \in \mathcal{S}_d$  be its discretized representation. Assume that each discretization bin has diameter at most  $\Delta$ , i.e.,

$$\|s - \omega(s_d)\| \leq \Delta,$$

where  $\omega(s_d)$  denotes a representative point (e.g., bin center) of  $s_d$ .

Define the optimal action in the continuous space and the discretized policy, respectively, as

$$\mathbf{a}^*(s) = \arg \max_{\mathbf{a} \in \mathcal{A}} \mu(s, \mathbf{a}), \quad \mathbf{a}_d^*(s_d) = \arg \max_{\mathbf{a} \in \mathcal{A}} \mu(\omega(s_d), \mathbf{a}).$$

Under Assumption 1, the performance loss due to discretization is bounded by

$$\mu(s, \mathbf{a}^*(s)) - \mu(s, \mathbf{a}_d^*(s_d)) \leq 2L\Delta. \quad (9)$$

*Proof.* Let  $\omega = \omega(s_d)$  be the representative point associated with the discretized state  $s_d$ . By Assumption 1, for any  $\mathbf{a} \in \mathcal{A}$ , we have

$$|\mu(s, \mathbf{a}) - \mu(\omega, \mathbf{a})| \leq L\|s - \omega\| \leq L\Delta. \quad (10)$$

By definition of  $\mathbf{a}^*(s)$ ,

$$\mu(s, \mathbf{a}^*(s)) \leq \mu(\omega, \mathbf{a}^*(s)) + L\Delta.$$

Since  $\mathbf{a}_d^*(s_d)$  maximizes  $\mu(\omega, \mathbf{a})$  over  $\mathcal{A}$ , we have

$$\mu(\omega, \mathbf{a}^*(s)) \leq \mu(\omega, \mathbf{a}_d^*(s_d)).$$

Applying the Lipschitz bound again,

$$\mu(\omega, \mathbf{a}_d^*(s_d)) \leq \mu(s, \mathbf{a}_d^*(s_d)) + L\Delta.$$

Combining the above inequalities yields

$$\mu(s, \mathbf{a}^*(s)) \leq \mu(s, \mathbf{a}_d^*(s_d)) + 2L\Delta,$$

which proves the result.  $\square$

Proposition 1 shows that the loss induced by discretizing the context space is controlled by the bin diameter  $\Delta$ . In particular, if the expected reward varies smoothly with respect to problem features (such as condition number and matrix norm), then finer discretizations lead to policies that approach the optimal continuous-context policy. This provides a theoretical justification for the discretization strategy used in our contextual bandit framework.

**Action Space Reduction** If the set of precisions is too large, then the size of the action space will exponentially increase, which significantly increases the training load. Let  $\mathcal{A}_1 = \{u_1, u_2, \dots, u_m\}$  be the set of precisions ordered by increasing significand bits. For the solver  $\mathcal{M}$  and  $k$  computational steps for which precisions must be selected, the action space  $\mathcal{A} = \mathcal{A}_1^k$  has cardinality  $m^k$ , where  $m$  is the number of precisions available to be chosen. To manage this exponential growth, we prune the action space by imposing a precision order constraint and limiting to the top- $k_{\text{top}}$  combinations.

Here, we write  $u_j < u_{j'}$  if  $u_j$  has fewer significand bits than  $u_{j'}$ . We enforce that the selected precisions for the  $k$  computational steps satisfy

$$u'_1 \leq u'_2 \leq u'_3 \leq \dots \leq u'_k, \quad u'_j \in \mathcal{A}_1 \quad (11)$$

This can naturally lead to valid precision combinations for some algorithms that is meaningful, as discussed in [33]. This idea is similar to modified delta-debugging in [31], which uses a greedy search approach instead of seeking a global minimum; it might miss potential reduced-precision configurations that suit the algorithm. The principle also naturally enables early stopping. For example, if precision  $u'_i$  fails, then it is not necessary to try a lower precision in step  $i$  or to try lower precision for steps  $j > i$  if it is already employed. Another benefit is that it allows users to define

the precision selection for the  $k$  computational steps in terms of their importance (the most important one is assigned to the last step  $k$ ). One benefit of using this strategy is to reduce the action space to

$$|\mathcal{A}_{\text{reduced}}| = \binom{m+k-1}{k} = \frac{(m+k-1)!}{k!(m-1)!}. \quad (12)$$

In the following experiments, we prune the action space from 256 to 35, a reduction of approximately 86%.

The exploration strategy is epsilon-greedy with linear decay. For episode  $t$ , the probability of selecting a random action from  $\mathcal{A}_{\text{reduced}}$  is

$$\epsilon_t = \max(\epsilon_{\min}, 1.0 - t/T). \quad (13)$$

This ensures exploration of lower-precision configurations early in training, shifting to exploitation of the best-known actions as  $\epsilon_t$  decreases. The reduced action space  $\mathcal{A}_{\text{reduced}}$  focuses on numerically stable configurations, accelerating convergence of the RL agent for the solver.

## 4 Case Study: GMRES-Based Iterative Refinement

### 4.1 Mixed-Precision GMRES-based Iterative Refinement

Iterative numerical methods, such as those for solving linear systems  $Ax = b$ , rely on a careful choice of arithmetic precisions to balance computational efficiency and numerical accuracy. The choice of precision for each computational step (e.g., working precision, residual computation) significantly impacts performance, yet optimal selection is challenging due to the complex dependence on system properties, such as condition number and sparsity. Traditional approaches often employ fixed or heuristic precision settings, which may lead to suboptimal performance across diverse problem instances. RL provides a data-driven approach to adaptively select precisions based on system characteristics, optimizing multiple objectives, such as residual norm and iteration count.

We instantiate the general RL framework for the GMRES-IR method [11], selecting precisions for four computational steps to solve linear systems  $Ax = b$ , reconciling the competing demands of numerical accuracy and computational efficiency. Consider a linear system  $Ax = b$ , where  $A \in \mathbb{R}^{n \times n}$  is non-singular, and  $b \in \mathbb{R}^n$ . GMRES-IR iteratively refines an initial solution  $x_0$  as:

$$x_{i+1} = x_i + z_i, \quad \text{where } Az_i = r_i,$$

and  $r_i = b - Ax_i$ . The system  $Az_i = r_i$  can be solved via preconditioned GMRES, i.e., we solve  $M^{-1}Az_i = M^{-1}r_i$ , where  $M \approx A$  is a preconditioner. In this study, we use the preconditioner  $M = LU$  (typically performed by backward and forward substitution) via LU factorization. The algorithm is presented in Algorithm 2. We refer to the loop in line 3 as *outer iterations* and the iterations within the GMRES solve in line 5 as *inner iterations*.

Our mixed-precision algorithms focus on four computational steps, each requiring a precision choice:

1. **LU Factorization and Initial Solution:** Compute  $M = LU \approx A$  and solve  $Mx_0 = b$  in precision  $u_f$ ,
2. **Residual Computation:** Compute the residual  $r_i = b - Ax_i$  in precision  $u_r$ .
3. **Working Precision for GMRES:** Solve  $M^{-1}Az_i = M^{-1}r_i$  using GMRES in precision  $u_g$ .
4. **Solution Update:** Compute  $x_{i+1} = x_i + z_i$  in precision  $u$ .

---

#### Algorithm 2 Mixed-precision GMRES based iterative refinement (GMRES-IR)

---

**Require:** an  $n \times n$  matrix  $A$  and a right-hand side  $b$ ;  $u_f$  is precision for factorization;

**Ensure:** Approximate solution  $\hat{x}$  to  $A\hat{x} = b$ .

- 1: Compute the LU factorization  $A = LU$ .  $u_f$
  - 2: Initialize  $x_0$  (to, e.g.,  $x_0 = U^{-1}L^{-1}(b)$ ).  $u_f$
  - 3: **for**  $i = 0, \dots$ , converged **do**
  - 4:   Compute  $r_i = b - Ax_i$ .  $u_r$
  - 5:   Solve  $U^{-1}L^{-1}Az_i = U^{-1}L^{-1}r_i$  using GMRES.  $u_g$
  - 6:   Compute  $x_{i+1} = x_i + z_i$ .  $u$
  - 7: **end for**
- 

It is worth noting that mixed precision can also be applied directly within the GMRES algorithm itself (see, for example, [33]). In this work, however, we limit our attention to GMRES implemented with a single, consistent precision for simplicity.

The goal is to use RL to select an action  $\mathbf{a} = (u_f, u, u_g, u_r)$  to minimize the final residual norm  $\|b - Ax_{\text{solve}}\|_2$  and the total number of iterations  $T$ , subject to a trade-off between  $T_{\text{max}}$  and the convergence tolerance  $\tau$ .

Inspired by stopping criteria from [14], we consider the algorithm converged if:

1. **Convergence:** The solver converges if the relative update norm is sufficiently small:

$$\frac{\|z_i\|_\infty}{\|x_i\|_\infty} \leq u_{\text{work}}, \quad (14)$$

where  $u_{\text{work}}$  is the unit roundoff for working precision, ensuring the update is on the order of the highest precision's roundoff error.

2. **Stagnation:** The solver stops if the update norms indicate insufficient progress:

$$\frac{\|z_i\|_\infty}{\|z_{i-1}\|_\infty} \geq \tau, \quad (15)$$

where  $\tau > 0$  is the stagnation tolerance, indicating that the updates are not changing significantly.

3. **Maximum Iterations:** The solver stops if the number of iterations reaches a predefined limit:

$$i \geq i_{\text{max}}, \quad (16)$$

where  $i_{\text{max}}$  is the maximum number of iterations.

To evaluate the accuracy and stability of the linear solve, we define the normwise relative forward error, and normwise relative backward error:

$$\text{ferr} = \frac{\|x_{\text{solve}} - x_{\text{true}}\|_\infty}{\|x_{\text{true}}\|_\infty}, \quad \text{nbe} = \frac{\|b - Ax_{\text{solve}}\|_\infty}{\|A\|_\infty \|x_{\text{solve}}\|_\infty + \|b\|_\infty}. \quad (17)$$

## 4.2 Contextual Bandit Formulation for Precision selection

The contextual bandit for the iterative refinement solver with preconditioned GMRES is defined by specifying the context, action, and reward components, tailored to optimize precision selection for solving linear systems  $Ax = b$ . The context, denoted  $s \in \mathbb{R}^d$ , where  $d = 2$ , captures properties of the linear system and is given by:

$$s = [\log_{10}(\max(\kappa(A), \delta_c)), \log_{10}(\max(\|A\|_\infty, \delta_n))], \quad (18)$$

where  $\kappa(A)$  is the condition number of  $A$  that can be approximated via an efficient algorithm (e.g., Hager-Higham [16, 18] and GNNs [9]),  $\delta_c > 0$  ensures numerical stability in logarithmic scaling,  $\|A\|_\infty = \max_i \sum_j |a_{ij}|$  is the infinity norm, and  $\delta_n > 0$  prevents numerical issues. These features characterize the numerical stability and scaling of the linear system and are fast to compute.

To learn the policy  $\pi$ , we employ a contextual bandit, discretizing the continuous state space  $\mathcal{S} \subset \mathbb{R}^d$  into a finite set to manage computational complexity. For each feature  $\phi_j$ ,  $j = 1, \dots, d$ , we define bins  $\Phi_j$ . The continuous state space  $\mathcal{S} \subset \mathbb{R}^d$  is discretized into a finite set  $\mathcal{S}_d$ , as in (3). For features  $\phi_1 = \log_{10}(\max(\kappa(A), \delta_c))$  and  $\phi_2 = \log_{10}(\max(\|A\|_\infty, \delta_n))$ , we define bins:

- $\Phi_1 = \log([\phi_{1,\text{min}}, \phi_{1,\text{max}}])$ , divided into  $n_1$  bins for the condition number (e.g., use approximate 1-norm).
- $\Phi_2 = \log([\phi_{2,\text{min}}, \phi_{2,\text{max}}])$ , divided into  $n_2$  bins for the matrix norm.

The discretized state space is  $\mathcal{S}_d = \Phi_1 \times \Phi_2$ , with cardinality  $|\mathcal{S}_d| = n_1 \cdot n_2$ . A state  $s_d \in \mathcal{S}_d$  is computed as:

$$s_d = \text{discretize}(s) = (\text{bin}(\phi_1(s)), \text{bin}(\phi_2(s))), \quad (19)$$

where  $\text{bin}(\phi_j(s))$  assigns  $\phi_j(s)$  to the nearest bin in  $\Phi_j$ , clipped to  $[0, |\Phi_j| - 1]$ . The state index is:

$$s_d = \text{bin}(\phi_1) \cdot n_2 + \text{bin}(\phi_2). \quad (20)$$

The action  $\mathbf{a} \in \mathcal{A}$  is a tuple  $\mathbf{a} = (u_f, u, u_g, u_r)$ ,  $u_i \in \mathcal{A}_1$  where  $\mathcal{A}_1 = \{u_1, \dots, u_m\}$  is the set of precisions, and  $m = |\mathcal{A}_1|$ . Following (12), the action space  $\mathcal{A}_{\text{reduced}} \subseteq \mathcal{A}$  is the top  $k$  elements of  $\mathcal{A} = \mathcal{A}_1^4$  is constrained by  $u_f \leq u \leq u_g \leq u_r$  where  $\leq$  denotes ordering by increasing significant bits.

The reward  $r(s, \mathbf{a})$  is designed to lead RL to choose precision configurations that lead the linear solvers to have an acceptable accuracy and number of iterations until convergence, it has the form:

$$R(s_d, \mathbf{a}) = w_2 f_{\text{precision}}(s_d, \mathbf{a}) + w_1 f_{\text{accuracy}}(s_d, \mathbf{a}) - f_{\text{penalty}}, \quad (21)$$

where the weights  $w_1, w_2 > 0$  balance accuracy and cost, and the individual components are defined as follows:

- **Precision term:**  $f_{\text{precision}}(s_d, \mathbf{a})$  encourages the use of lower-precision formats based on their significant bits. For each precision  $p \in \{u_f, u, u_g, u_r\}$ , the cost is weighted by the ratio of significant bits relative to FP64:

$$f_{\text{precision}}(s_d, \mathbf{a}) = \sum_{p \in \{u_f, u, u_g, u_r\}} \frac{t_{\text{FP64}}}{t_p(1 + \log_{10}(\max(\kappa, 1)))}, \quad (22)$$

where  $t_u$  is the number of significant bits for precision  $u$ , and  $\kappa$  is the condition number of the matrix  $\mathbf{A}$ .

- **Accuracy term:** To define the accuracy term, we further refine the error terms based on (17):

$$\text{err}_{\text{distance}} = \frac{\|x_{\text{solve}} - x_{\text{true}}\|_{\infty}}{\|x_{\text{true}}\|_{\infty}}, \quad \text{err}_{\text{normalized}} = \frac{\text{ferr}}{\|A\|_{\infty}\|x_{\text{true}}\|_{\infty} + \|b\|_{\infty}}, \quad (23)$$

where  $x_{\text{solve}}$  is the solution obtained by the reinforcement learning policy,  $x_{\text{true}}$  is the ground-truth solution or high-precision reference solution (here we use the one computed in FP64),  $\|A\|_{\infty}$  is the matrix infinity norm, and small constants can be added in denominators to prevent division by zero.

$f_{\text{accuracy}}(s_d, \mathbf{a})$  penalizes the error in the solution relative to the true solution and the normalized residual. We define the accuracy-related reward as a piecewise function based on the forward and normalized backward errors:

$$f_{\text{accuracy}}(s_d, \mathbf{a}) = -C_1 (\min(\log_{10}(\max(\text{ferr}, \varepsilon)), \theta) + \min(\log_{10}(\max(\text{nbe}, \varepsilon)), \theta)), \quad (24)$$

where  $\text{ferr}$  and  $\text{nbe}$  are defined in (17),  $\varepsilon$  is a small constant (e.g.,  $10^{-10}$ ), and  $\theta > 0$  is a truncation threshold that limits the reward when the errors are large. Often, setting  $\theta = 2.5$  is applicable to most cases.

- **Penalty:** We use the term  $f_{\text{penalty}}$  to denote the penalty arising from computational cost, e.g., iterations or failure steps such as LU factorization or stagnation calculation. In our empirical study, it is sufficient to use the converged iterations to model the penalty term; that is, the more iterations we use, the larger the penalty term will be. In this context, we can either use the total number of iterations for iterative refinement or the total (inner-solve) GMRES iterations used for iterative refinement, denoted by  $T_{\text{iter}}$ . The following definition is used in our context:

$$f_{\text{penalty}} = \log_2(\max(T_{\text{iter}}, 1)), \quad (25)$$

which can be also used in other linear solve. One can also enforce a weight  $w_3$  on this term to avoid hiding the effect of other terms during training.

We use a contextual bandit update for a single Q-table  $Q : \mathcal{S}_d \times \mathcal{A} \rightarrow \mathbb{R}$ . Actions are selected using an epsilon-greedy strategy with

$$\epsilon_t = \max(\epsilon_{\min}, 1.0 - t/T), \quad (26)$$

as in Section 3.2. The Q-table is updated as

$$Q(s_d, \mathbf{a}) \leftarrow Q(s_d, \mathbf{a}) + \alpha (R(s_d, \mathbf{a}) - Q(s_d, \mathbf{a})), \quad \mathbf{a} \in \mathcal{A}_{\text{reduced}}. \quad (27)$$

The precision selection RL framework specialized for GMRES-IR is presented in Algorithm 3. It applies RL to a training set of  $N$  linear systems, selecting precisions via an epsilon-greedy strategy and updating the Q-table based on solver performance. The GMRES method is adapted to handle mixed-precision computations, with the preconditioner applied in precision  $u_g$ .

## 5 Experiments

We conducted experiments to evaluate the proposed RL framework for precision selection in GMRES-IR for solving linear systems  $p = (A, b) \in \mathcal{P}$ , where  $A \in \mathbb{R}^{n \times n}$  is a non-singular matrix and  $b \in \mathbb{R}^n$ . The systems are derived from random generated matrices. Our code is simulated in Python and uses Pychop [8] for precision emulation.

We generated problems  $Ax = b$  using two settings, each designed to evaluate the RL-driven precision selection for the GMRES-IR solver under different numerical conditions versus a full double precision routine (in the following, we use FP64 and double precision interchangeably). The agent with learning rate  $\alpha$  of 0.5 is trained within a custom Gym environment [4] with 100 episodes, which simulates the process of solving a linear system using the GMRES-IR solver. To reduce the action space and accelerate computation, we adopted the reduction strategy outlined in Section 3.2 and further pruned it by selecting one-fourth of the valid precision combinations from the episode number combinations.

In the following experiments, we evaluate the resulting relative forward errors (as defined in (17)), the number of iterative refinement iterations required for convergence, and the total number of inner GMRES iterations required for convergence. All the computed results for the relative forward and backward errors (abbreviated as error in the tables and figures for simplicity in the following) are preserved to 2 significant digits. For a fair comparison, we set the same convergence tolerance  $\tau$  for both RL baseline and the reference baseline.

**Algorithm 3** Contextual Bandit Learning for GMRES-IR Precision Selection

- 
- 1: **Input:** Training systems  $\{(A_j, b_j)\}_{j=1}^N$ , GMRES-IR method  $\mathcal{M}$ , precision set  $\mathcal{A}_1 = \{u_1, \dots, u_m\}$ , reward function  $r$ , episodes  $T$ , tolerance  $\tau$ , max iterations  $T_{\max}$ , learning rate  $\alpha$ , minimum exploration probability  $\epsilon_{\min}$ , bins  $\{\Phi_1, \Phi_2\}$ , top- $k$  parameter  $k_{\text{top}}$
  - 2: Compute  $\mathcal{A}_{\text{reduced}}$  in terms of  $\mathcal{A} = \mathcal{A}_1^4$  with  $k_{\text{top}}$  elements satisfying (11)
  - 3: Initialize tabular action-value estimator  $Q(s_d, \mathbf{a})$  for  $s_d \in \mathcal{S}_d$ ,  $\mathbf{a} \in \mathcal{A}_{\text{reduced}}$
  - 4: Initialize environment  $\mathcal{E}$  with systems  $\{(A_j, b_j)\}$
  - 5: **for** episode  $t = 1$  to  $T$  **do**
  - 6:   **for** system  $(A_j, b_j)$ ,  $j = 1, \dots, N$  **do**
  - 7:     Compute context  $s_j = \lceil \log_{10}(\max(\kappa(A_j), \delta_c)), \log_{10}(\max(\|A_j\|_{\infty}, \delta_n)) \rceil$
  - 8:     Discretize state  $s_d = \text{discretize}(s_j, \{\Phi_1, \Phi_2\})$
  - 9:     Compute  $\epsilon_t = \max(\epsilon_{\min}, 1.0 - t/T)$
  - 10:     Select action  $\mathbf{a} = (u_f, u, u_g, u_r) \in \mathcal{A}_{\text{reduced}}$  via:
 
$$\mathbf{a} = \begin{cases} \text{random choice from } \mathcal{A}_{\text{reduced}}, & \text{if with } \epsilon_t \text{ probability,} \\ \arg \max_{\mathbf{a}' \in \mathcal{A}_{\text{reduced}}} Q(s_d, \mathbf{a}'), & \text{otherwise.} \end{cases}$$
  - 11:     Solve  $A_j x = b_j$  with  $\mathcal{M}$  using  $\mathbf{a}$ :
  - 12:     Compute  $M = LU \approx A_j$  in precision  $u_f$
  - 13:     Solve  $M x_0 = b_j$  in precision  $u_f$
  - 14:     **for**  $l = 0$  to  $T_{\max} - 1$ :
    - 15:       Compute  $r_l = b_j - A_j x_l$  in precision  $u_r$
    - 16:       Solve  $M^{-1} A_j z_l = M^{-1} r_l$  using GMRES with in precision  $u_g$
    - 17:       Update  $x_{l+1} = x_l + z_l$  in precision  $u$
    - 18:       **if** stopping criteria is met or failure occurs: **break**
    - 19:       Compute reward  $r(s_j, \mathbf{a})$  per (21)
    - 20:       Update tabular action-value estimator:
 
$$Q(s_d, \mathbf{a}) \leftarrow Q(s_d, \mathbf{a}) + \alpha (R(s_d, \mathbf{a}) - Q(s_d, \mathbf{a}))$$
  - 21:     **end for**
  - 22: **end for**
  - 23: **Inference:** For new system  $(A, b)$ , compute  $s = \lceil \log_{10}(\max(\kappa(A), \delta_c)), \log_{10}(\max(\|A\|_{\infty}, \delta_n)) \rceil$ , discretize  $s_d$ , select  $\mathbf{a} = \arg \max_{\mathbf{a} \in \mathcal{A}_{\text{reduced}}} Q(s_d, \mathbf{a})$ , solve with  $\mathcal{M}$  using  $\mathbf{a}$
- 

**5.1 Problem Setup**

To ensure sufficient diversity in the data, we synthetically generated the linear systems, comprising  $N_{\text{train}}$  training and  $N_{\text{test}}$  testing systems  $\{\mathcal{P}_i = (A_i, b_i)\}_{i=1}^{N_{\text{train}} + N_{\text{test}}}$ . The data generation iterated until  $N_{\text{train}} + N_{\text{test}} = 200$  systems were obtained. Specifically, we set  $N_{\text{train}} = 100$  training and  $N_{\text{test}} = 100$  testing systems. The generation process incorporates randomization for matrix sizes (between 100 and 500) and condition number ( $10^1, 10^9$ ) to ensure diversity in matrix structures, enforcing variability in numerical stability. This diversity is critical for evaluating our RL-based precision selection strategy. We use precision set  $\mathcal{U} = \{\text{BF16, TF32, FP32, FP64}\}$  and the discretized state as in (3), based on two features:  $\phi_1 = \log_{10}(\max(\kappa(A), \delta_c))$  (condition number) and  $\phi_2 = \log_{10}(\max(\|A\|_{\infty}, \delta_n))$  (matrix norm), where  $\delta_c, \delta_n > 0$  ensure numerical stability. These features  $\Phi_1$  and  $\Phi_2$  are separately binned into 10 bins ( $n_1 = n_2 = 10$ ), respectively and their minimum and maximum value in terms of the training set. The discretized state space is  $\mathcal{S}_d = \Phi_1 \times \Phi_2$ , with cardinality  $|\mathcal{S}_d| = n_1 \cdot n_2$ , and states are indexed as in (3).

To evaluate the performance of the RL-based solver  $\mathcal{M}$ , we define the success rate across a test set of linear systems  $\{\mathcal{P}_1, \dots, \mathcal{P}_M\} \subset \mathcal{S}$ . For each system  $\mathcal{P} = (A, b)$ , the solver produces a solution  $x_{\text{rl}}$  using the learned policy  $\pi$ .

The performance is assessed using the following error metrics maximum error `ferr` and nbe, defined by:

$$\epsilon_{\max}(\mathcal{P}, \mathbf{a}) = \max(\text{ferr}, \text{nbe}).$$

For each condition number range  $\mathcal{R}j$ , a threshold is defined:

$$\tau_j = \tau_{\text{base}} \cdot \text{median}(\kappa(A) \mid \mathcal{P} = (A, b) \in \mathcal{R}j), \quad (28)$$

where  $\tau_{\text{base}} > 0$  is the base tolerance. A system  $\mathcal{P} \in \mathcal{R}j$  is considered successfully solved if:

$$\epsilon_{\max}(\mathcal{P}, \mathbf{a}) < \tau_j. \quad (29)$$

To evaluate the proportion of systems that achieve acceptable accuracy, the success rate  $\xi_j$  for the range  $\mathcal{R}_j$  is:

$$\xi_j = \frac{|\mathcal{P} \in \mathcal{R}_j \mid \epsilon \max(\mathcal{P}, \mathbf{a}) < \tau_j|}{|\mathcal{R}_j|}, \quad (30)$$

where  $|\mathcal{R}_j|$  is the cardinality  $\mathcal{R}_j$ , and the threshold  $\tau_j$  is scaled by the condition number to account for problem difficulty, aligning with the error bounds in [14].

To comprehensively assess the performance of our approach and study the hyperparameters, we choose the precision types of BF16, TF32, FP32, and FP64 for exploration and simulate our models with two weight settings  $W_1$  and  $W_2$  for (21);  $W_1$  indicates  $w_1 = 1, w_2 = 0.1$ , and  $W_2$  indicates  $w_1 = w_2 = 1.0$ . Compared to  $W_1$ , the setting  $W_2$  increases the value of second weight parameter, and is expected to enable the model to choose the lower precision more aggressively.

The following simulations evaluate performance using the success rate  $\xi$ , the normative relative forward error (`ferr`), the normative relative backward error (`nbe`), and the iteration count, with comparisons against an FP64 baseline. All the *Avg. ferr*, *Avg. nbe*, *Avg iter*. and *Avg GMRES iter*. in the tables are separately calculated from the average value of `ferr`, `nbe`, converged iterations for iterative refinement, and total GMRES iterations used for inner solve from all samples, respectively. The reward and the average Reward Prediction Error (RPE) per episode during training are shown in the Appendix.

## 5.2 Simulations on Dense Systems

We generated linear systems with varying condition numbers and matrix sizes for training and testing sets, following MATLAB’s gallery(‘randsvd’) function with mode=2. These datasets are created using a singular value decomposition approach. The synthetic sets test solvers with mixed-precision configurations determined by RL. This allows us to verify the reinforcement learning agent’s robustness in selecting precision strategies for systems that exhibit variability. For a matrix  $A \in \mathbb{R}^{n \times n}$ , we construct:

$$A = U \Sigma V^T,$$

where  $U, V \in \mathbb{R}^{n \times n}$  are orthogonal matrices obtained via QR decomposition of random matrices with entries drawn from a standard normal distribution, and  $\Sigma = \text{diag}(\sigma_1, \sigma_2, \dots, \sigma_n)$  is a diagonal matrix with the singular values.

The singular values are:

$$\sigma_k = \begin{cases} \sigma_{\max}, & k = 1, 2, \dots, n-1, \\ \sigma_{\max}/\kappa, & k = n, \end{cases} \quad (31)$$

where  $\sigma_{\max} > 0$  is the largest singular value and  $\kappa \geq 1$  is the desired condition number, ensuring  $\kappa(A) = \sigma_1/\sigma_n = \kappa$ . The singular values are sorted in descending order ( $\sigma_1 = \sigma_2 = \dots = \sigma_{n-1} = \sigma_{\max} \geq \sigma_n = \sigma_{\max}/\kappa$ ), resulting in a dense matrix  $A$  with the specified condition number  $\kappa(A) = \kappa$ . The ground-truth solution  $x \in \mathbb{R}^n$  is generated with entries independently sampled from a standard normal distribution, and the right-hand side vector  $b = Ax$ .

Table 2 reports error metrics and iteration counts for the linear solve, organized by condition number ranges: low ( $10^0$  to  $10^3$ ), medium ( $10^3$  to  $10^6$ ), and high ( $10^6$  to  $10^9$ ). Figure 2 details the precision types selected within finer condition number intervals.

Regarding convergence, the conservative  $W_1$  policy achieves universal convergence with a descent success rate  $\xi = 100\%$  across all settings. In comparison, the aggressive  $W_2$  policy maintains 100% success at  $\tau = 10^{-6}$  but shows reduced robustness at the stricter tolerance  $\tau = 10^{-8}$ , with  $\xi$  decreasing to 89.2% in the low- $\kappa$  tests (RL fails in a few test samples). This is likely because the RL had insufficient exposure to training data in this specific range.

With respect to accuracy,  $W_1$  closely matches the FP64 baseline, producing forward errors of the same order of magnitude and comparable backward errors. Precision lower than FP32 is never used in  $W_1$ . By contrast,  $W_2$  exhibits a clear trade-off: BF16 and TF32 start to be used within low-to-medium  $\kappa$  ranges, which is consistent with the fact that smaller condition numbers theoretically permit lower-precision computations with decreased error amplification. The  $W_2$  policy permits the use of low precisions with substantially higher errors (e.g., `ferr`  $\approx 10^{-7}$ ) to optimize the reward function, as long as the convergence quality is guaranteed.

This behavioral distinction also shows up in computational effort. The average number of outer iterations remains stable ( $\approx 2.0$  to 2.35) for both policies. However, the inner solver cost varies. The  $W_2$  policy requires slightly more inner GMRES iterations (e.g., 8.00 compared to 2.70 for  $W_1$  in low- $\kappa$  bins). This increase is needed to offset the growing rounding errors introduced by lower-precision formats.

The visualization of `ferr` and total GMRES iterations used for each test sample in  $W_2$  is shown in Figure 3. The average performance degradation in Table 2 for the  $W_2$  policy stems from a few instances that deviate from the identity line due to its aggressive strategy, favoring reduced precision.

Table 2: Average Performance Metrics Across Condition Ranges for Dense Systems.

Method	Condition Range	$\xi$	Avg. ferr	Avg. nbe	Avg iter.	Avg. GMRES iter.
$\tau = 10^{-6}$						
RL( $W_1$ )	Low ( $10^0$ – $10^3$ )	100%	$1.19 \times 10^{-14}$	$7.90 \times 10^{-17}$	2.35	2.70
	Medium ( $10^3$ – $10^6$ )	100%	$1.57 \times 10^{-11}$	$2.82 \times 10^{-15}$	2.26	2.20
	High ( $10^6$ – $10^9$ )	100%	$1.89 \times 10^{-9}$	$1.63 \times 10^{-14}$	2.21	2.54
RL( $W_2$ )	Low ( $10^0$ – $10^3$ )	100%	$2.48 \times 10^{-7}$	$2.19 \times 10^{-8}$	2.30	8.00
	Medium ( $10^3$ – $10^6$ )	100%	$4.22 \times 10^{-7}$	$4.95 \times 10^{-11}$	2.29	3.40
	High ( $10^6$ – $10^9$ )	100%	$1.89 \times 10^{-9}$	$1.63 \times 10^{-14}$	2.21	2.54
<b>FP64 Baseline (<math>\tau = 10^{-6}</math>)</b>						
	Low ( $10^0$ – $10^3$ )	–	$1.20 \times 10^{-14}$	$7.96 \times 10^{-17}$	2.00	2.00
	Medium ( $10^3$ – $10^6$ )	–	$1.46 \times 10^{-11}$	$8.13 \times 10^{-17}$	2.00	2.00
	High ( $10^6$ – $10^9$ )	–	$1.92 \times 10^{-9}$	$8.09 \times 10^{-17}$	2.00	2.00
$\tau = 10^{-8}$						
RL( $W_1$ )	Low ( $10^0$ – $10^3$ )	100%	$1.18 \times 10^{-14}$	$7.40 \times 10^{-17}$	2.35	4.49
	Medium ( $10^3$ – $10^6$ )	100%	$2.95 \times 10^{-11}$	$9.60 \times 10^{-13}$	2.14	4.77
	High ( $10^6$ – $10^9$ )	100%	$2.02 \times 10^{-9}$	$7.93 \times 10^{-17}$	2.11	3.79
RL( $W_2$ )	Low ( $10^0$ – $10^3$ )	89.2%	$2.49 \times 10^{-7}$	$2.61 \times 10^{-8}$	2.22	9.54
	Medium ( $10^3$ – $10^6$ )	100%	$3.49 \times 10^{-6}$	$6.44 \times 10^{-11}$	2.14	4.71
	High ( $10^6$ – $10^9$ )	100%	$3.91 \times 10^{-6}$	$4.28 \times 10^{-11}$	2.11	3.57
<b>FP64 Baseline (<math>\tau = 10^{-8}</math>)</b>						
	Low ( $10^0$ – $10^3$ )	–	$1.20 \times 10^{-14}$	$7.96 \times 10^{-17}$	2.00	2.00
	Medium ( $10^3$ – $10^6$ )	–	$1.46 \times 10^{-11}$	$8.13 \times 10^{-17}$	2.00	2.00
	High ( $10^6$ – $10^9$ )	–	$1.92 \times 10^{-9}$	$8.14 \times 10^{-17}$	2.00	2.93

The precision selection patterns in Figure 2 clarify these performance outcomes. In the low- $\kappa$  range ( $10^0$  to  $10^3$ ),  $W_1$  employs a conservative combination of FP64 and FP32, entirely avoiding lower precisions. In contrast,  $W_2$  leverages BF16 and TF32 (with usage frequencies of approximately 0.33 and 0.76, respectively), reflecting a focus on cost-efficiency. As the condition number increases, both strategies converge; beyond  $10^6$ , both policies adopt an FP64-dominant strategy and avoid the use of lower precisions.

Although our RL framework for precision selection tolerates a loss of accuracy, the primary finding is that the RL agent develops an intelligent condition-dependent precision-adaptation strategy. It utilizes lower-precision formats (BF16/TF32) to achieve computational efficiency in well-conditioned systems, particularly under the  $W_2$  policy, but transitions decisively to high-precision FP64 as the matrix becomes ill-conditioned. This behavior demonstrates that the RL agent internalizes theoretical constraints on backward error growth and dynamically prioritizes numerical stability over computational speed when problem difficulty increases.

### 5.3 Simulations on Sparse Systems

In this simulation, we emulated sparse linear systems following the experiment described in [17]. A matrix  $A_0 \in \mathbb{R}^{n \times n}$  is constructed with  $\text{nnz}(A_0) = \lfloor \lambda_s n^2 \rfloor$  non-zero entries, where  $\lambda_s > 0$  is the sparsity parameter. The entries are sampled from a standard normal distribution:

$$a_{ij} \sim \mathcal{N}(0, 1), \quad (i, j) \in \{(r_k, c_k)\}_{k=1}^{\text{nnz}(A_0)},$$

where  $r_k, c_k \in \{1, \dots, n\}$  are randomly chosen indices. The matrix is symmetrized and made positive definite:

$$A = A_0 A_0^T + \beta I,$$

where  $\beta > 0$  is a diagonal shift and  $I$  is the identity matrix. The same as the tests for dense linear systems, the ground-truth solution  $x \in \mathbb{R}^n$  is generated with entries independently sampled from a standard normal distribution,

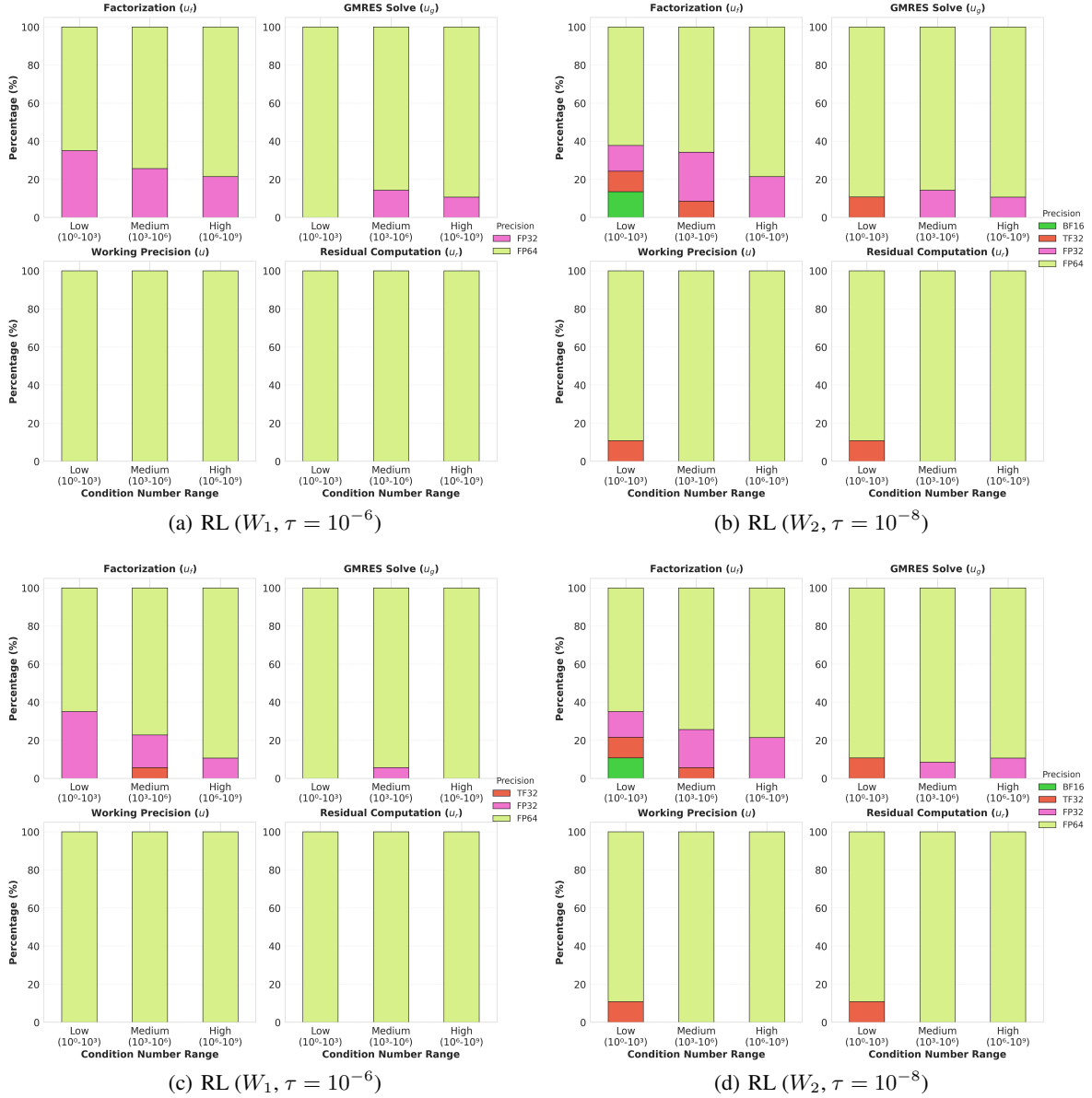


Figure 2: Average Floating-point Types Selected Across Low, Medium, and High Condition Ranges.

and the right-hand side vector  $b = Ax$ . For all problems, matrices have non-zero diagonal entries ( $a_{ii} \neq 0$ ) and are non-singular.

Table 3: Train/Test Metrics Summary

Metric	Train (min – max)	Test (min – max)
Condition number	$9.926 \times 10^7 - 1.559 \times 10^{10}$	$1.016 \times 10^8 - 7.863 \times 10^9$
Sparsity	1.80% – 5.10%	1.80% – 5.00%
Matrix size	103 – 500	100 – 498

Setting  $\lambda_s = 0.01$ , the random sparse linear systems in our training set and testing set following the above generation routines are described in Table 3. Similar to the above (under the same evaluation metrics, two tolerance levels, and two reward weight policies), Table 4 showcases the average performance of the RL-guided mixed-precision iterative

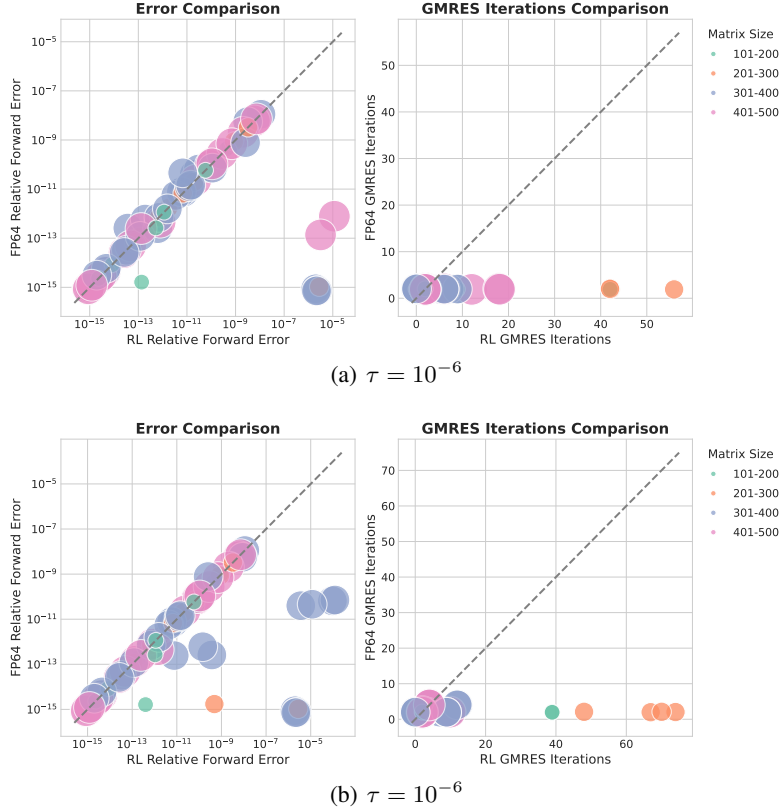


Figure 3: Comparison of RL and FP64 in terms of errors and iteration counts. Marker colors denote different matrix-size groups, while marker sizes represent the number of test samples in each group.

refinement solver on sparse linear systems. Table 5 details the average selection frequency of four floating-point formats across the four precision-controlled stages, with each row summing to 4.

Table 4: Average Performance Metrics for Sparse Systems.

Method	$\xi(\%)$	Avg. ferr	Avg. nbe	Avg Iter.	Avg. GMRES iter.
$\tau = 10^{-6}$					
RL ( $W_1$ )	100.00	$4.91 \times 10^{-9}$	$5.26 \times 10^{-17}$	2.01	2.22
RL ( $W_2$ )	100.00	$4.91 \times 10^{-9}$	$5.26 \times 10^{-17}$	2.01	2.22
FP64 Baseline	–	$4.90 \times 10^{-9}$	$5.28 \times 10^{-17}$	2.00	2.00
$\tau = 10^{-8}$					
RL ( $W_1$ )	100.00	$4.90 \times 10^{-9}$	$5.28 \times 10^{-17}$	2.00	2.10
RL ( $W_2$ )	100.00	$4.91 \times 10^{-9}$	$5.28 \times 10^{-17}$	2.01	2.36
FP64 Baseline	–	$4.90 \times 10^{-9}$	$5.28 \times 10^{-17}$	2.00	2.10

The evaluation of sparse linear systems presents a distinct contrast to the dense case, primarily driven by the inherent numerical difficulty posed by the very ill-conditioned dataset. As depicted in Table 3, the test matrices exhibit high condition numbers between  $1.02 \times 10^8$  and  $7.86 \times 10^9$ , which places linear solve in a range where numerical stability is precarious, leaving limited room for precision reduction. This test effectively demonstrates whether the RL agent can effectively avoid numerical instabilities in its precision selection.

Table 4 summarizes the performance metrics. Under these harsh conditions, the RL agent exhibits a highly conservative behavior. Regardless of the reward weight setting ( $W_1$  or  $W_2$ ) or the tolerance level ( $\tau$ ), the agent achieves a 100%

Table 5: Average Floating-point Precision Usage Per Solve for Sparse Systems.

Weight Setting	BF16	TF32	FP32	FP64
$\tau = 10^{-6}$				
RL ( $W_1$ )	0.00	0.00	0.01	3.99
RL ( $W_2$ )	0.00	0.00	0.01	3.99
$\tau = 10^{-8}$				
RL ( $W_1$ )	0.00	0.00	0.00	4.00
RL ( $W_2$ )	0.00	0.00	0.01	3.99

success rate with error metrics (ferr and nbe) that are close to the FP64 baseline. Unlike the dense case, where  $W_2$  triggered an increase in GMRES iterations to trade off lower precision, here the average iteration counts (both outer and GMRES) for RL policies align closely with the baseline. This indicates that the agent has learned that any reduction in precision, even for the sake of potential reward, would likely lead to stagnation or divergence.

This conservative approach is further quantified in Table 5. The precision distribution indicates a consistent reliance on double precision, with FP64 usage averaging approximately 3.99 to 4.00 steps per solve. Even under the aggressive weighting scheme  $W_2$ , which strongly incentivizes low-precision usage, the agent entirely avoids selecting BF16 and TF32. This convergence of  $W_1$  and  $W_2$  strategies is a significant finding: it demonstrates that the RL agent correctly identifies the "survival boundary" of the iterative method. When faced with uniformly ill-conditioned sparse systems, the policy effectively overrides the efficiency-driven incentives of  $W_2$  and prioritizes the fundamental necessity of numerical convergence. Thus, the framework proves robust, defaulting to a high-precision fallback when the problem's spectral properties render low-precision formats numerically unsafe.

#### 5.4 Study on Iteration Penalty

The limitation of precision tuning in linear solvers without accounting for convergence iterations often comes with the most dynamic precision tuning tools like HiFPTuner [15] because they focus only on precision tuning with the restriction on accuracy.

To further verify the effectiveness of our RL modeling for precision selection and performance balance, we further conduct a reward component analysis to evaluate the contribution of the penalty term. We focus on the total converged GMRES iterations taken for iterative refinement and conduct an ablation study on training with (21) without the penalty  $f_{\text{penalty}}$  in the iteration terms.

The results are presented in Table 6, together with Figure 4 showing precision types chosen by RL. Similarly to above, we observed that between low- and medium-conditioned linear systems, RL strategically selects aggressive reduced-precision steps, whereas in high-conditioned linear systems it adopts a more conservative strategy for precision selection. Compared to the training with  $f_{\text{penalty}}$  as shown in Figure 2, the one without the  $f_{\text{penalty}}$  leads to more reduced-precision actions. The removal of it  $f_{\text{penalty}}$  results in increasing iterations for the RL agent to achieve comparable accuracy, which means the iterative refinement uses extra iterations to compensate for the accuracy loss resulting from using increased low-precision steps. The results indicate the importance of the reward function modeling for RL training and demonstrate the effectiveness of RL for precision selection under proper reward modeling.

## 6 Discussion

Unlike supervised learning problem, such as classification, our contextual bandit RL framework is more well-suited for practical solve since it does not require ground-truth labels, which is of more practical to numerical analysis problems. However, our RL framework for precision selection requires proper state modeling of the data. For instance, we use features such as the approximate condition number and matrix norm in our state modeling for the linear solve problem. Selecting or modeling the states often requires expert knowledge to balance reasonable computational complexity with sufficient information for effective RL training.

However, this limitation, on the other hand, can also be viewed as an advantage. In this work, the proposed framework has shown efficient precision selection even when prior knowledge about the required precision for critical computational steps is lacking. Although prior studies have explored mixed-precision usage in iterative refinement methods based on condition numbers and matrix sizes, our framework offers two unique benefits. First, it can quickly determine the

Table 6: Average Performance Metrics Across Condition Ranges for Dense Systems (remove penalty on iteration).

Method	Condition Range	$\xi$	Avg. ferr	Avg. nbe	Avg iter.	Avg. GMRES iter.
$\tau = 10^{-6}$						
RL( $W_1$ )	Low ( $10^0$ – $10^3$ )	100%	$8.86 \times 10^{-8}$	$1.45 \times 10^{-10}$	2.65	11.05
	Medium ( $10^3$ – $10^6$ )	100%	$4.22 \times 10^{-7}$	$4.97 \times 10^{-11}$	2.54	5.94
	High ( $10^6$ – $10^9$ )	100%	$1.94 \times 10^{-9}$	$1.63 \times 10^{-14}$	2.32	3.25
RL( $W_2$ )	Low ( $10^0$ – $10^3$ )	100%	$3.37 \times 10^{-7}$	$2.20 \times 10^{-8}$	2.46	12.08
	Medium ( $10^3$ – $10^6$ )	100%	$4.22 \times 10^{-7}$	$4.97 \times 10^{-11}$	2.54	5.94
	High ( $10^6$ – $10^9$ )	100%	$1.94 \times 10^{-9}$	$1.63 \times 10^{-14}$	2.32	3.25
<b>FP64 Baseline (<math>\tau = 10^{-6}</math>)</b>						
	Low ( $10^0$ – $10^3$ )	–	$1.20 \times 10^{-14}$	$7.96 \times 10^{-17}$	2.00	2.00
	Medium ( $10^3$ – $10^6$ )	–	$1.46 \times 10^{-11}$	$8.13 \times 10^{-17}$	2.00	2.00
	High ( $10^6$ – $10^9$ )	–	$1.92 \times 10^{-9}$	$8.09 \times 10^{-17}$	2.00	2.00
$\tau = 10^{-8}$						
RL( $W_1$ )	Low ( $10^0$ – $10^3$ )	100%	$1.34 \times 10^{-11}$	$1.62 \times 10^{-12}$	2.38	15.97
	Medium ( $10^3$ – $10^6$ )	100%	$3.49 \times 10^{-6}$	$6.44 \times 10^{-11}$	2.31	12.37
	High ( $10^6$ – $10^9$ )	100%	$3.91 \times 10^{-6}$	$4.28 \times 10^{-11}$	2.11	3.57
RL( $W_2$ )	Low ( $10^0$ – $10^3$ )	89.2%	$2.49 \times 10^{-7}$	$2.61 \times 10^{-8}$	2.27	21.03
	Medium ( $10^3$ – $10^6$ )	100%	$3.49 \times 10^{-6}$	$6.48 \times 10^{-11}$	2.34	12.51
	High ( $10^6$ – $10^9$ )	100%	$3.91 \times 10^{-6}$	$4.28 \times 10^{-11}$	2.18	4.29
<b>FP64 Baseline (<math>\tau = 10^{-8}</math>)</b>						
	Low ( $10^0$ – $10^3$ )	–	$1.20 \times 10^{-14}$	$7.96 \times 10^{-17}$	2.00	2.00
	Medium ( $10^3$ – $10^6$ )	–	$1.46 \times 10^{-11}$	$8.13 \times 10^{-17}$	2.00	2.00
	High ( $10^6$ – $10^9$ )	–	$1.92 \times 10^{-9}$	$8.14 \times 10^{-17}$	2.00	2.93

required precision for unseen linear systems. Second, it allows us to identify the required precision for selected matrix features in a black-box setting. For example, by selecting certain features in our state space, we can examine whether these features are key factors (salient or not) that determine the reduced mixed precision. When the salient features are unknown or when their influence on the required precision level is unclear, our framework becomes particularly advantageous.

## 7 Conclusion and Future Work

We present a reinforcement learning framework for automated precision selection in linear solvers, casting the problem as a contextual bandit that balances convergence across iterations and low precision usage. Using iterative refinement as a case study, the framework dynamically adjusts precision at different computation steps to better balance numerical accuracy and efficiency. Our empirical results show that RL, leveraging a discretized state space, effectively adapts precision choices to the numerical properties of each linear system and achieves a good compromise between algorithm performance (relative error and converged iterations) and the reduced-precision portion of the linear systems under varying conditions.

In the future, we will explore deep RL for continuous-state spaces, incorporate additional significant matrix features (e.g., fill-in ratio, pivot growth estimates, sparsity, and spectral properties), and examine their contributions to improving the method’s performance by reducing precision. By addressing these, we will be able to extend this framework to a broader range of numerical algorithms to advance the mixed-precision techniques.

## References

- [1] A. Abdelfattah, H. Anzt, E. G. Boman, E. Carson, T. Cojean, J. Dongarra, A. Fox, M. Gates, N. J. Higham, X. S. Li, J. Loe, P. Luszczek, S. Pranesh, S. Rajamanickam, T. Ribizel, B. F. Smith, K. Swirydowicz, S. Thomas,

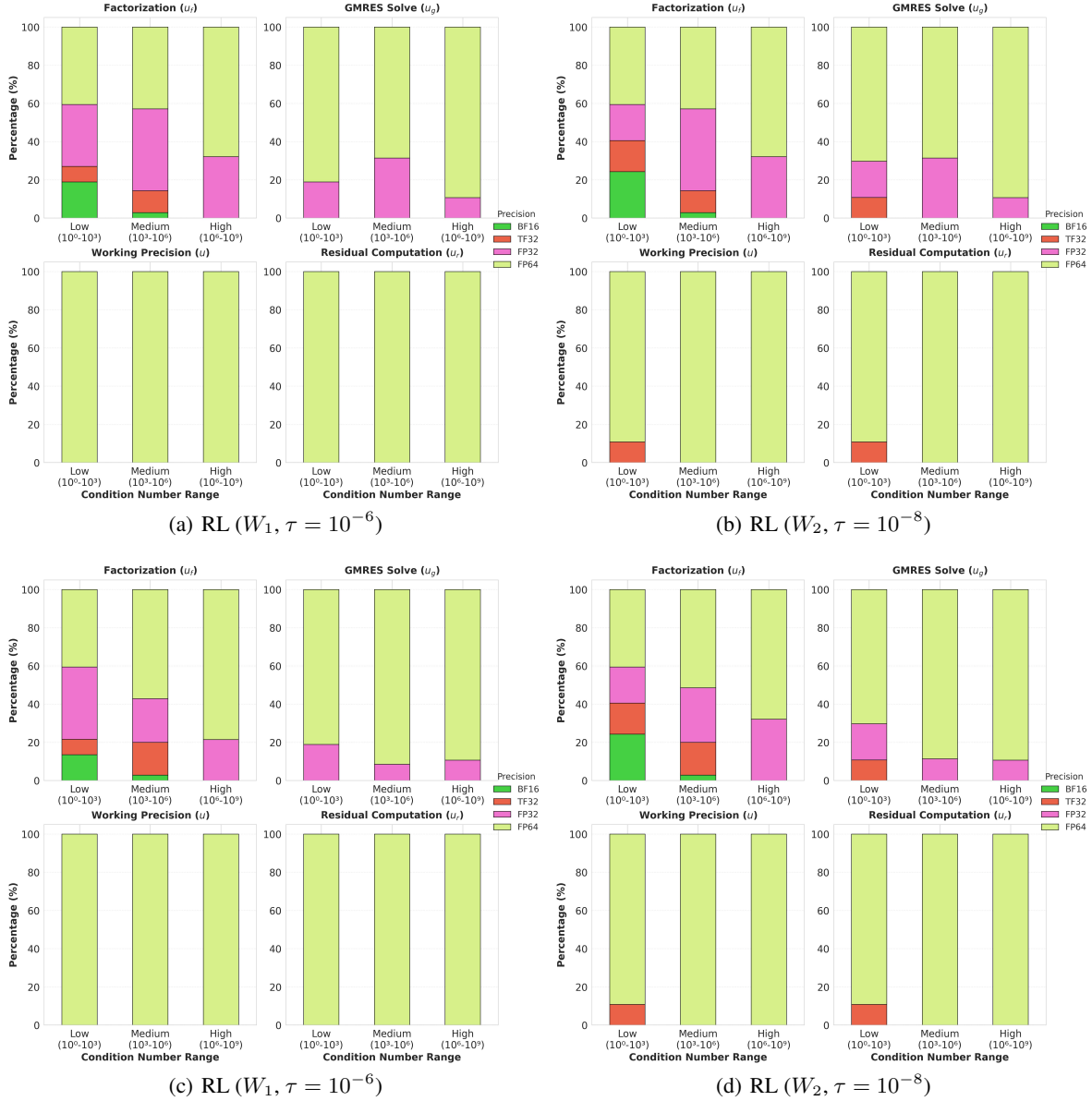


Figure 4: Average Floating-point Types Selected Across Low, Medium, and High Condition Ranges (remove penalty on iteration).

- S. Tomov, Y. M. Tsai, and U. M. Yang. A survey of numerical linear algebra methods utilizing mixed-precision arithmetic. *The International Journal of High Performance Computing Applications*, 35(4):344–369, 2021.
- [2] P. R. Amestoy, A. Buttari, N. J. Higham, J.-Y. L’Excellent, T. Mary, and B. Vieublé. Five-Precision GMRES-based Iterative Refinement. *SIAM J. Matrix Anal. Appl.*, 45(1):529–552, 2024.
- [3] D. Ben Khalifa and M. Martel. Everything you Need to Know About Reduced Mixed Precision Computation in Numerical Programs, 2023.
- [4] G. Brockman, V. Cheung, L. Pettersson, J. Schneider, J. Schulman, J. Tang, and W. Zaremba. OpenAI Gym, 2016.
- [5] T. B. Brown, B. Mann, N. Ryder, M. Subbiah, J. Kaplan, P. Dhariwal, A. Neelakantan, P. Shyam, G. Sastry, A. Askell, S. Agarwal, A. Herbert-Voss, G. Krueger, T. Henighan, R. Child, A. Ramesh, D. M. Ziegler, J. Wu, C. Winter, C. Hesse, M. Chen, E. Sigler, M. Litwin, S. Gray, B. Chess, J. Clark, C. Berner, S. McCandlish, A. Radford, I. Sutskever, and D. Amodei. Language models are few-shot learners. *CoRR*, abs/2005.14165, 2020.

- [6] H. Brunie, C. Iancu, K. Z. Ibrahim, P. Brisk, and B. Cook. Tuning floating-point precision using dynamic program information and temporal locality. In *SC20: International Conference for High Performance Computing, Networking, Storage and Analysis*, pages 1–14, 2020.
- [7] B. Buck and J. K. Hollingsworth. An API for runtime code patching. *Int. J. High Perform. Comput. Appl.*, 14(4):317–329, 2000.
- [8] E. Carson and X. Chen. Pychop: Emulating low-precision arithmetic in numerical methods and neural networks, 2025.
- [9] E. Carson and X. Chen. Estimating condition number with graph neural networks, 2026.
- [10] E. Carson and N. J. Higham. A new analysis of iterative refinement and its application to accurate solution of ill-conditioned sparse linear systems. *SIAM Journal on Scientific Computing*, 39(6):A2834–A2856, 2017.
- [11] E. Carson and N. J. Higham. Accelerating the solution of linear systems by iterative refinement in three precisions. *SIAM Journal on Scientific Computing*, 40(2):A817–A847, 2018.
- [12] E. Carson, N. J. Higham, and S. Pranesh. Three-precision gmres-based iterative refinement for least squares problems. *SIAM Journal on Scientific Computing*, 42(6):A4063–A4083, 2020.
- [13] S. Cherubin and G. Agosta. Tools for reduced precision computation: A survey. *ACM Comput. Surv.*, 53(2), Apr. 2020.
- [14] J. Demmel, Y. Hida, W. Kahan, X. S. Li, S. Mukherjee, and E. J. Riedy. Error bounds from extra-precise iterative refinement. *ACM Trans. Math. Softw.*, 32(2):325–351, 2006.
- [15] H. Guo and C. Rubio-González. Exploiting community structure for floating-point precision tuning. In *Proceedings of the 27th ACM SIGSOFT International Symposium on Software Testing and Analysis, ISSTA 2018*, pages 333–343, USA, 2018. ACM.
- [16] W. W. Hager. Condition estimates. *SIAM Journal on Scientific and Statistical Computing*, 5(2):311–316, 1984.
- [17] P. Häusner, O. Öktem, and J. Sjölund. Neural incomplete factorization: learning preconditioners for the conjugate gradient method. *Transactions on Machine Learning Research*, 2024.
- [18] N. J. Higham. A survey of condition number estimation for triangular matrices. *SIAM Review*, 29(4):575–596, 1987.
- [19] N. J. Higham and S. Pranesh. Exploiting lower precision arithmetic in solving symmetric positive definite linear systems and least squares problems. *SIAM Journal on Scientific Computing*, 43(1):A258–A277, 2021.
- [20] E. J. Hu, yelong shen, P. Wallis, Z. Allen-Zhu, Y. Li, S. Wang, L. Wang, and W. Chen. LoRA: Low-rank adaptation of large language models. In *International Conference on Learning Representations*, 2022.
- [21] IEEE. IEEE standard for floating-point arithmetic. *IEEE Std 754-2019 (Revision of IEEE 754-2008)*, pages 1–84, 2019.
- [22] Y. Jang, P. Jolivet, and T. Mary. Mixed Precision Augmented GMRES. working paper or preprint, July 2025.
- [23] M. O. Lam and J. K. Hollingsworth. Fine-grained floating-point precision analysis. *Int. J. High Perform. Comput. Appl.*, 32(2):231–245, 2018.
- [24] P. Micikevicius, S. Narang, J. Alben, G. F. Diamos, E. Elsen, D. García, B. Ginsburg, M. Houston, O. Kuchaiev, G. Venkatesh, and H. Wu. Mixed precision training. *CoRR*, abs/1710.03740, 2017.
- [25] P. Micikevicius, D. Stosic, N. Burgess, et al. FP8 formats for deep learning, 2022.
- [26] C. B. Moler. Iterative refinement in floating point. *J. ACM*, 14(2):316–321, Apr. 1967.
- [27] NVIDIA Corporation. NVIDIA A100 Tensor Core GPU Architecture. <https://www.nvidia.com/content/dam/en-zz/Solutions/Data-Center/a100/pdf/nvidia-a100-datasheet.pdf>, 2020.
- [28] E. Oktay and E. Carson. Multistage mixed precision iterative refinement. *Numerical Linear Algebra with Applications*, 29(4):e2434, 2022.
- [29] H. Peng, K. Wu, Y. Wei, G. Zhao, Y. Yang, Z. Liu, Y. Xiong, Z. Yang, B. Ni, J. Hu, R. Li, M. Zhang, C. Li, J. Ning, R. Wang, Z. Zhang, S. Liu, J. Chau, H. Hu, and P. Cheng. FP8-LM: Training fp8 large language models, 2023.
- [30] C. Rubio-González, C. Nguyen, B. Mehne, K. Sen, J. Demmel, W. Kahan, C. Iancu, W. Lavrijsen, D. H. Bailey, and D. Hough. Floating-point precision tuning using blame analysis. In *IEEE/ACM 38th International Conference on Software Engineering*, pages 1074–1085, 2016.
- [31] C. Rubio-González, C. Nguyen, H. D. Nguyen, J. Demmel, W. Kahan, K. Sen, D. H. Bailey, C. Iancu, and D. Hough. Precimonious: Tuning assistant for floating-point precision. In *SC '13: Proceedings of the International Conference on High Performance Computing, Networking, Storage and Analysis*, pages 1–12, 2013.

- 
- [32] H. Touvron, T. Lavril, G. Izacard, X. Martinet, M.-A. Lachaux, T. Lacroix, B. Rozière, N. Goyal, E. Hambro, F. Azhar, A. Rodriguez, A. Joulin, E. Grave, and G. Lample. Llama: Open and efficient foundation language models, 2023.
  - [33] B. Vieublé. Mixed precision iterative refinement for the solution of large sparse linear systems, Nov. 2022.
  - [34] Y. Wang and C. Rubio-González. Predicting performance and accuracy of mixed-precision programs for precision tuning. In *Proceedings of the IEEE/ACM 46th International Conference on Software Engineering, ICSE '24, USA, 2024*. ACM.
  - [35] J. H. Wilkinson, R. S. Martin, G. Peters, and H. J. Bowdler. Solution of real and complex systems of linear equations. *Numerische Mathematik*, 8(3):217–234, 1966.
  - [36] Q. Xu, T. Mytkowicz, and N. S. Kim. Approximate computing: A survey. *IEEE Design & Test*, 33(1):8–22, 2016.

## Training Rewards and Loss

### .1 For Dense Linear Systems

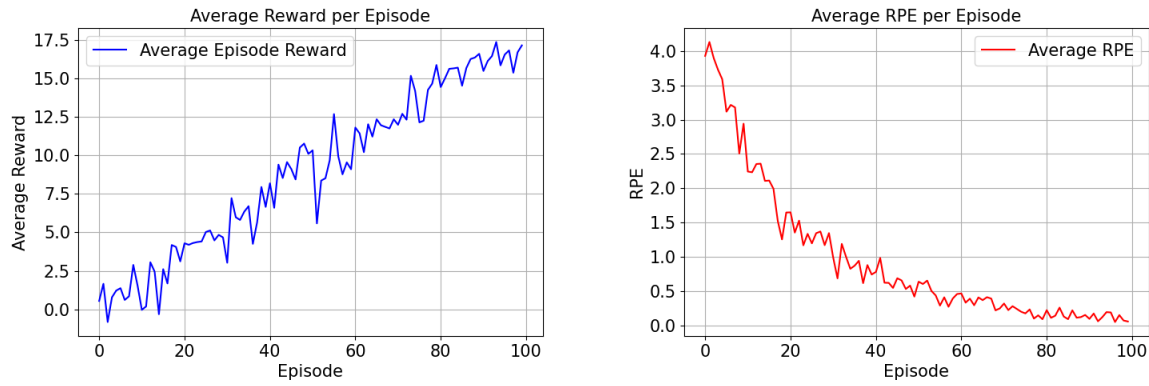


Figure 5:  $RL(W_1), \tau = 10^{-6}$

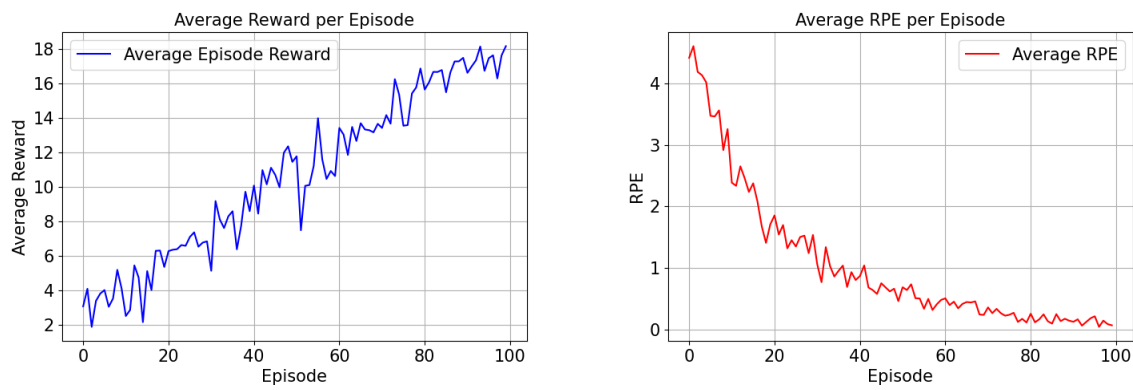


Figure 6:  $RL(W_2), \tau = 10^{-6}$

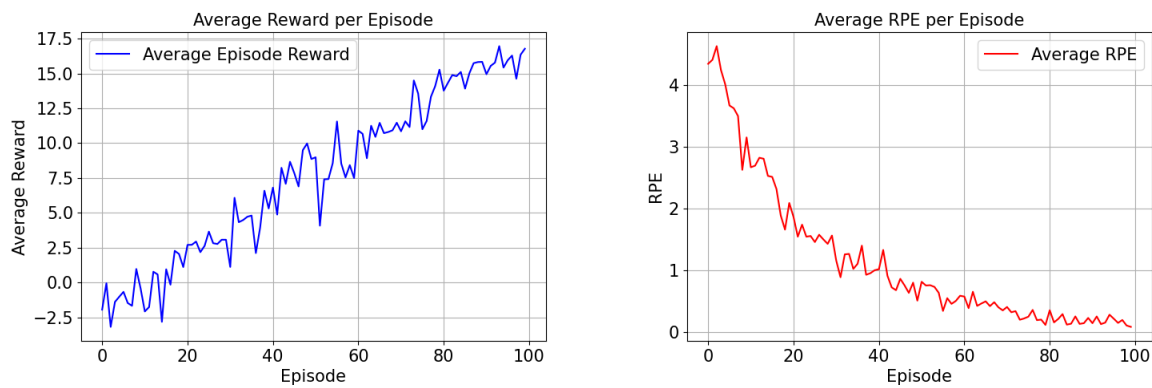
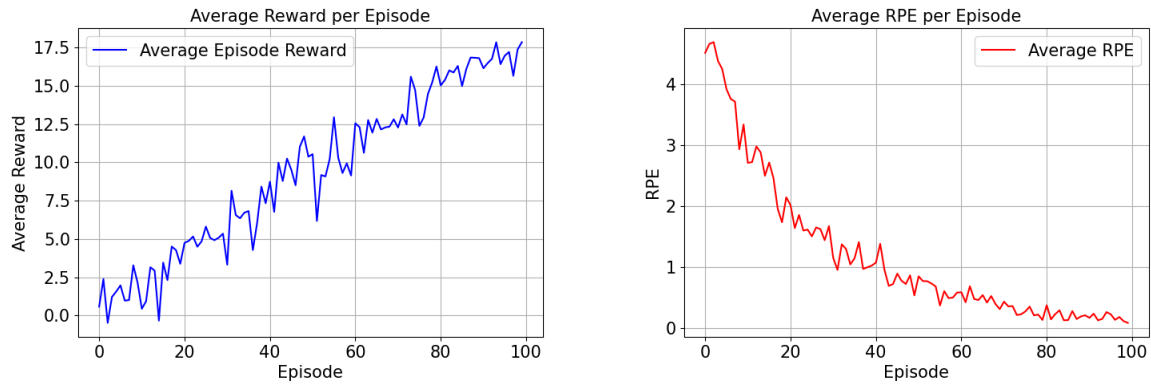
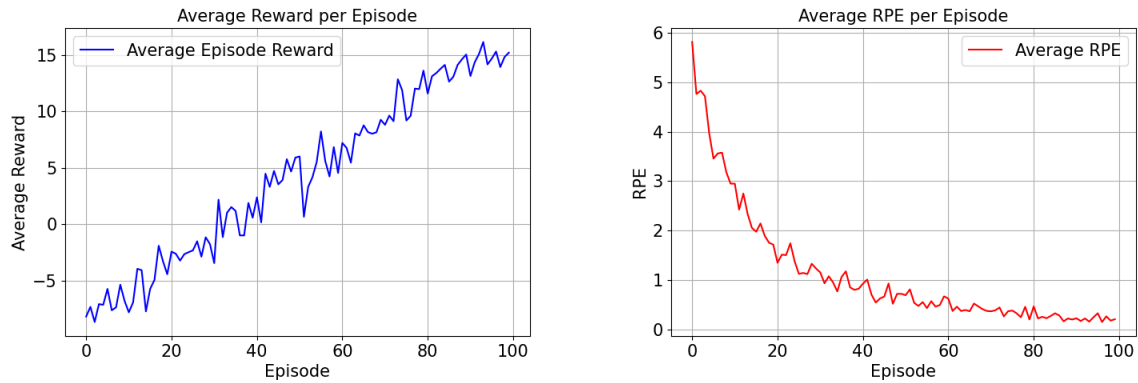
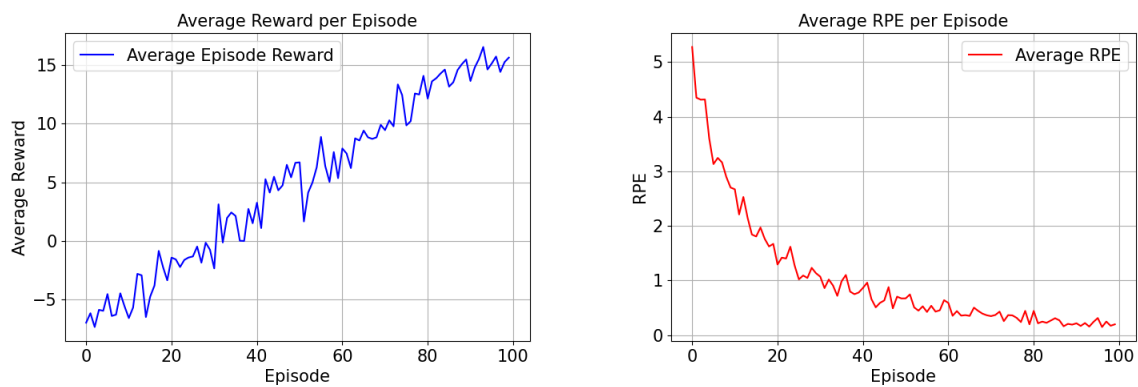
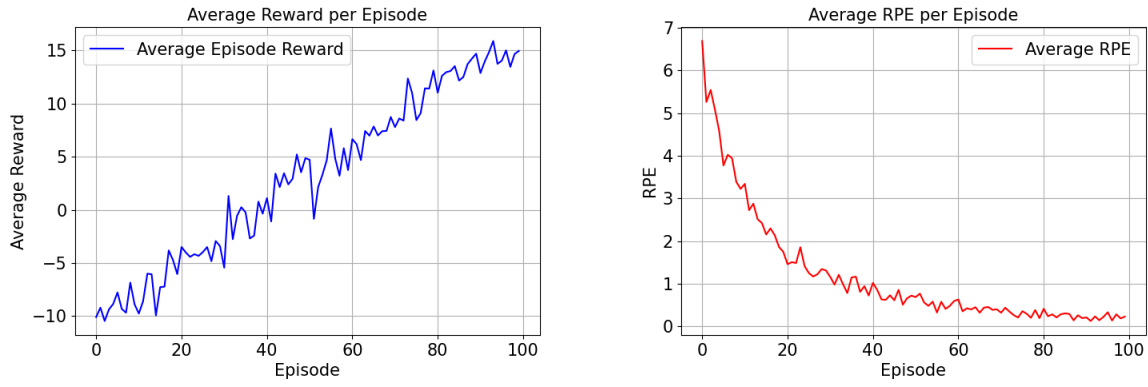
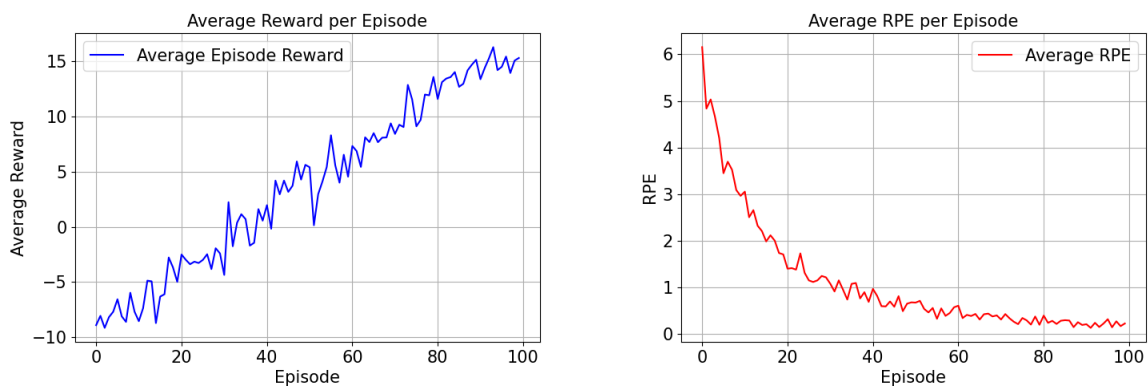


Figure 7:  $RL(W_1), \tau = 10^{-8}$

Figure 8:  $RL(W_2), \tau = 10^{-8}$ 

## 2 For Sparse Linear Systems

Figure 9:  $RL(W_1), \tau = 10^{-6}$ Figure 10:  $RL(W_2), \tau = 10^{-6}$

Figure 11:  $RL(W_1)$ ,  $\tau = 10^{-8}$ Figure 12:  $RL(W_2)$ ,  $\tau = 10^{-8}$